SOIL SCIENCE ANNUAL
2025, 76(3), 211370

https://doi.org/10.37501/soilsa/211370

Micromorphological, submicromorphological and chemical indicators of pedogenesis in Spolic Technosols developed at historical mining and metallurgical sites in the Tatra Mountains, southern Poland

Magdalena Tarnawczyk[a*], Łukasz Uzarowicz[a], Artur Pędziwiatr[a], Wojciech Kwasowski[a]

[a] Warsaw University of Life Sciences – SGGW, Institute of Agriculture, Department of Soil Science, Nowoursynowska Str. 159, building no. 37, 02-776 Warsaw, Poland

* Corresponding author: Magdalena Tarnawczyk, MSc. Eng., magdalena_tarnawczyk@sggw.edu.pl, ORCID iD: https://orcid.org/0000-0001-7324-0812

Received: 2025-08-09
Accepted: 2025-09-26
Published online: 2025-09-26
Associated editor: Cezary Kabała

Keywords:

Spolic Technosols
Soil-forming processes
Soil micromorphology
Mountain soils
Historical mining
Historical smelting

Abstract

Spolic Technosols developed from mine and metallurgical wastes in areas of historical mining and smelting activities undergo natural weathering, soil-forming and biological processes. This study presents (1) micromorphological and submicromorphological features using optical microscopy and scanning electron microscopy, as well as (2) chemical characteristics based on selective extractions of pedogenic Fe, Al, Mn and Si in Technosols from the Tatra Mountains, southern Poland, to identify key pedogenic processes in these soils. This approach provides insight into the complex pedogenesis of Spolic Technosols in an alpine environment influenced by past industrial activity. Thirteen soil profiles were analysed, divided into three groups: (I) Technosols formed from mine wastes comprising Fe- and Mn-ore-bearing carbonate rocks (limestones and dolomites), (II) Technosols developed from mine wastes derived from polymetallic ore-bearing igneous and metamorphic rocks (granite, gneiss), and (III) Technosols containing wastes from smelting activity (e.g. metallurgical slags). Soil thin section analysis revealed the following microscale evidences of initial soil formation: (1) formation of Fe oxide pseudomorphs due to sulphide weathering; (2) formation of pedogenic structure; (3) formation of pedogenic carbonate coatings in soils developed from mine wastes composed of carbonate rocks; (4) formation of pedogenic Fe and Mn oxide coatings in acidic soils developed from mine wastes composed of crystalline rocks (granite, gneiss); (5) formation of pedogenic sulphate coatings in soils containing metallurgical wastes, and (6) bioturbations (e.g. root channels and biogenic channels filled with a material reworked by soil animals). Micromorphological observations also showed that metallurgical slags in Technosols can serve as a habitat for soil fauna (most likely nematodes or enchytraeids). Selective extractions of pedogenic Fe, Al, Mn, and Si showed (1) the release of oxalate-extractable Mn in soils developed from Mn-bearing ore mine wastes, (2) a slight mobilisation of oxalate-extractable Fe and Al in acidic Technosols developed from aluminosilicate parent material, and (3) the release of oxalate-extractable Al and Si in Technosols containing metallurgical slags. These results indicate that technogenic parent materials undergo weathering, which will most likely consequently transform the mineral composition of the studied Technosols in the future. This study contributes to expanding knowledge of Technosols and their potential ecological functions in mountain regions. It also provides insights into soil development in areas of historical mining and metallurgical activities in an alpine environment of the Tatra Mountains.

1. Introduction

The study of soils in areas affected by historical human activities provides valuable insights into pedogenic processes and the long-term environmental effects of anthropogenic disturbances. Technosols, recognised by the World Reference Base for Soil Resources (IUSS Working Group WRB, 2022), are characterised by the presence of artefacts that are human-made, human-altered, and human-excavated materials (Charzyński et al., 2013; Uzarowicz et al., 2020a). Important soils among them are Spolic Technosols, which develop, for example, at disposal sites containing mine and industrial wastes (Néel et al.,

2003; Kabała et al., 2020; Swęd et al., 2022). These soils are commonly found in contemporary industrial areas (Grünewald et al., 2007; Uzarowicz et al., 2017; Allory et al., 2022). However, they also occur in places of historical industrial activity, which nowadays are often covered with vegetation due to natural plant succession (Woś et al., 2023; Castillo Corzo et al., 2025; Uzarowicz et al., 2025). Sometimes, these areas can comprise ecologically sensitive environments and protected areas. An example of such a site is the Tatra Mountains, currently protected as the Tatra National Park.

The Tatra Mountains, part of the Western Carpathians, are a high mountain area in southern Poland and northern Slovakia with a long history of mining and metallurgical activity (Jost, 2004; Rączkowska, 2019). Mining and metallurgy in the Tatra Mountains lasted from the 15th century until the end of the 19th century (Radwańska-Paryska and Paryski, 1995), with the greatest environmental impact in the 18th and early 19th centuries (Zwoliński, 1984). Mining and metallurgy activities have left a legacy of altered landscapes as well as mine wastes and metallurgical slags deposited on the land surface, affecting biodiversity and soil quality (Mirek, 1996). These anthropogenic materials are unique soil substrates from which Spolic Technosols develop after covering a post-industrial area with vegetation. Although the properties and geochemical features of Technosols in historical metal mining and smelting areas in the Tatra Mountains were recently identified and described (Tarnawczyk et al., 2024, 2025), the advancement of soil-forming processes in these soils is still poorly recognised. Therefore, there is a need to extend our knowledge about soil development in abandoned mining and smelting areas. This combined micromorphological and chemical approach provides novel insights into soil-forming processes in high-mountain Technosols, which have not been studied in detail in the Tatra Mountains before.

Micromorphological analysis, which aims to recognise soil characteristics at the micro-scale, in addition to chemical analyses on pedogenic forms of Fe, Al, Mn, and Si, offers a valuable tool for studying the effects of early soil-forming processes in Technosols. In the last two decades, soil micromorphology has become more and more frequently used to study the genesis of Technosols (Zikeli et al., 2002; Zanuzzi et al., 2009; Séré et al., 2010; Uzarowicz and Skiba, 2011; Jangorzo et al., 2013; Huot et al., 2015; Uzarowicz et al., 2017, 2018b; Watteau et al., 2017; Ortega et al., 2022). Recent micromorphological studies (e.g., Huot et al., 2014b; Watteau et al., 2018, 2025; Colombini et al., 2020; Ruiz et al., 2022; Díaz-Ortega et al., 2024) have focused on the investigation of pedogenic processes in human-affected soils of industrial regions in lowland and upland areas. However, comparable data from high mountain environments are scarce. Identifying micromorphological features of the groundmass, soil organic matter, and pedofeatures reveals the interplay between anthropogenic influences and natural soil-forming processes (Zaiets and Poch, 2016; Stoops et al., 2018; Verrecchia and Trombino, 2021). Previous studies on soil micromorphology in the Tatra Mountains, such as those by Zasoński and Niemyska-Łukaszuk (1977), Miechówka and Ciarkowska (1998), and Drewnik (2008), have primarily focused on the determination of properties of natural (non-anthropogenic) soils; however, soils in the areas affected by historical mining and smelting activities have not been investigated.

Selective extractions of Fe, Al, Si, and Mn from soils are frequently used to differentiate mineralogical and chemical forms of Fe, Al, Si, and Mn in soils, as well as to assess pedogenic transformations and mineral weathering, which is helpful in identifying the degree of advancement of soil-forming processes and in distinguishing between different soil types (McKeague and Day, 1966; Cornell and Schwertmann, 2003). Selective extractions of Fe, Al, Si, and Mn for Technosols developed from different anthropogenic parent materials (thermal power station ash, mine wastes containing Fe and Cu sulphides; mine wastes from sedimentary Fe ore mines) indicate the release of these elements in soil environment and proves that the results of the extractions can be a good indicator of initial soil-forming processes in Technosols (Uzarowicz and Skiba, 2011; Uzarowicz et al., 2017, 2024, 2025). It seems that the selective extractions of Fe, Al, Si, and Mn should also be used for Technosols developed from other anthropogenic parent materials, including technogenic soils of the Tatra Mountains.

The purpose of this study was to determine the degree of advancement of soil-forming processes in Spolic Technosols developed at historical mining and metallurgical sites in the Tatra Mountains (southern Poland), based on micromorphological, submicromorphological, and chemical indicators of pedogenesis. We hypothesised that (1) micromorphological and submicromorphological features, together with pedogenic forms of Fe, Al, Si, and Mn, can be used to trace the intensity and direction of soil-forming processes over several centuries of Technosol development, and (2) these features provide insights into the genesis of high-mountain Technosols and their ecological implications in human-influenced mountain ecosystems.

2. Materials and methods

2.1. Study area

The study was conducted in the Tatra Mountains, the highest range of the Carpathians, located in southern Poland along the border with Slovakia. This region is characterised by an alpine environment, with elevations ranging from approximately 900 to 2500 meters above sea level. The climatic conditions are harsh, with the mean annual air temperatures ranging from 6°C in the valleys to –4°C near the peaks, and the mean annual precipitation from 1000 mm in the lowest part up to 1800 mm in the highest part of the mountains (Hess, 1996).

The Tatra Mountains are part of the Western Carpathians and consist predominantly of granitoids in the High Tatras and metamorphic rocks in the Western Tatras, as well as sedimentary rocks in the lower part of the Western Tatras (Kotański, 1971; Passendorfer, 1996; Gradziński et al., 2001). The relief of the Tatra Mountains is shaped by glacial, fluvial, and slope processes, creating a complex landscape of valleys and ridges (Klimaszewski, 1996).

The Tatra Mountains are a typical alpine environment with distinct altitudinal vegetation zones. The lowest zone, up to about 1250 m a.s.l., is dominated by beech (*Fagus sylvatica* L.) and fir (*Abies alba* Mill.), while spruce (*Picea abies* (L.) H. Karst) is also widespread due to past forest management. Between 1250 and 1550 m a.s.l., the upper forest belt develops, dominated by spruce and silver birch (*Betula pendula* Roth). Above, in the subalpine zone (1550–1800 m a.s.l.), the main component of the vegetation is dwarf pine (*Pinus mugo* Turra) scrub. At an altitude of 1800–2300 m a.s.l., alpine grasslands predominate, with species such as *Juncus trifidus* and *Festuca varia*, while above 2300 m a.s.l., the subnival zone is characterised by lichens, mosses, and low grasses in harsh climatic conditions (Piękoś-Mirkowa and Mirek, 1996).

The mosaic pattern is very characteristic of the soil cover in the Tatra Mountains (Komornicki and Skiba, 1996). The soils have diverse properties depending mostly on parent rock (various igneous, sedimentary, and metamorphic rocks), vegetation, morphogenetic processes, and climatic conditions (Komornicki and Skiba, 1996). The most common soils occurring in the Tatra Mountains are Podzols, rendzina soils (Rendzic Leptosols), brown soils (Cambisols), as well as initial soils (Leptosols and Regosols) (Komornicki and Skiba, 1996; Drewnik et al., 2008).

Historical mining and metallurgical activities, conducted particularly from the medieval period to the end of the 19th century, have locally influenced the region's soil substrates (Osika, 1987; Jost, 2004). The remnants of these activities are, for example, mine waste heaps and slag disposal sites, which serve as parent materials for Spolic Technosols investigated in the present study.

2.2. Study object

The study focuses on Spolic Technosols developed in areas of historical mining and metallurgy in the Tatra Mountains. These soils were formed from anthropogenic substrates including mine waste and metallurgical slags originating from the extraction and processing of copper (Cu), iron (Fe), silver (Ag), manganese (Mn), and antimony (Sb) ores (Wątocki, 1950; Jost, 1962, 2004). In the Polish part of the Tatra Mountains, mining activity developed mainly in the Western Tatras (the Chochołowska and Kościeliska Valley region, including the Ornak ridge), whereas the metallurgical centres were located in Kuźnice and the Kościeliska Valley (Liberak, 1927).

Thirteen soil profiles from eight selected sites located on small heaps at adit outlets, near collapsed adits and shafts, and in historical smelting areas were examined. Detailed location of the soil profiles, including a map and images of representative profiles with surrounding vegetation, was presented elsewhere (Tarnawczyk et al., 2024). The profiles were located at the following sites: (a) the Huciańskie Banie (profiles 1 and 2); (b) mouth of the Kościeliska Valley (profile 3); (c) the Kościeliska Valley near the Ornak tourist shelter (profile 4); (d) the Pyszniańska Valley (profiles 5 and 6); (e) the Żleb pod Banie (Pod Banie Couloir) at the Ornak ridge (profiles 7 and 8); (f) the Banisty Żleb (Banisty Couloir) at the Ornak ridge (profiles 9 and 10); (g) the Kościeliska Valley – old steelwork at Stare Kościeliska (profiles 11 and 12); and (h) Kuźnice steelwork area (profile 13). The periods of activity of the studied mining and smelting sites are listed in Tarnawczyk et al. (2024). These sites reflect the variability in parent material petrology, mineral composition, soil properties, and differences in vegetation cover. Soil samples were taken from each horizon distinguished in the soil profiles.

The studied soils were classified as different variants of Spolic Technosols or Coarsic Spolic Technosols (Tarnawczyk et al., 2024) (Table 1), following the guidelines of the World Reference Base for Soil Resources (IUSS Working Group WRB, 2022). These soils were grouped based on their properties and the character of parent materials (Tarnawczyk et al., 2024). Group I includes Technosols formed from mine wastes comprising Fe- and Mn-ore-bearing carbonate rocks (limestones and dolomites), represented by profiles 1–3. Group II comprises Technosols developed from mine wastes derived from polymetallic ore-bearing igneous and metamorphic rocks (granite, gneiss), represented by profiles 5–10. Group III includes Technosols containing metallurgical wastes (e.g., slags), represented by profiles 11–13. Profile 4 combines the properties of group I and II. The age of soils was estimated based on information about the time of the operation of a mine or smelter at each study site (Jost, 2004) (Table 1). We suppose that the soils began to develop after the deposition of mine or metallurgical wastes on the land surface.

2.3. Laboratory analyses

2.3.1. Soil properties

The basic physicochemical properties of the studied Technosols were determined in accordance with standard pedological procedures (Van Reeuwijk, 2002; Pansu and Gautheyrou, 2006; Soil Science Division Staff, 2017). Soil samples from each horizon were air-dried, sieved to a size of <2 mm, and analysed for particle size distribution (Bouyoucos–Casagrande method, modified by Prószyński) (Warzyński et al., 2018), pH (potentiometric, H_2O, 1:2.5), carbonate content (Scheibler volumetric method), total organic carbon (TOC), total nitrogen (TN), and total sulphur (TS) using a CHNS elemental analyser (vario MACRO cube, Elementar). In carbonate-containing samples, inorganic C was subtracted from TOC. The mass-specific magnetic susceptibility (χ) was measured with a multifunction MFK1-FA Kappabridge, following Thompson and Oldfield (1986). A full description of the methodology and results is provided in Tarnawczyk et al. (2024). These parameters provide an essential background for the micromorphological study.

2.3.2. Micromorphological analyses

The undisturbed samples were collected from the selected soil horizons. The samples were then air-dried and impregnated with Araldite 2020 epoxy resin. Polished thin sections with a thickness of 30 μm were prepared from the impregnated soil materials at the Faculty of Geology, University of Warsaw, Poland. They were examined in transmitted light using petrographic microscopes (Olympus SZX Z10, Olympus BX41). The micromorphological description and terminology given by Stoops (2021) were applied.

Table 1
Selected physical and chemical properties of the studied soils based on Tarnawczyk et al. (2024)

Horizon	Depth (cm)	Munsell colour (moist)*	Rock fragments (%)*	Percentage of fractions (mm)			Soil textural class (USDA)	Magnetic susceptibility (χ) ($\times 10^{-8} \cdot m^3 \cdot kg^{-1}$)	pH_{H2O}	eq. $CaCO_3$ (%)	TOC (%)	TN (%)	TS (%)
				2.0–0.05	0.05–0.002	< 0.002							
Profile 1 – *Spolic Technosol (Loamic, Eutric, Calcaric, Humic, Hyperartefactic, Skeletic, Toxic)* Approximate time of soil origin: late 18th c. – mid-19th c.													
Oi	0–1	10YR 2/2	–	–	–	–	–	–	–	–	42.40	1.46	0.10
AC1	1–5	10YR 3/1	15	76	17	7	SL	83.5	7.4	20.5	8.19	0.56	0.08
AC2	5–15	10YR 3/2	60	76	15	9	SL	91.4	7.9	31.2	2.18	0.12	0.04
C	15–35	2.5YR 3/3	70	75	15	10	SL	36.8	8.0	30.4	1.85	0.07	0.04
2C	35–60	10YR 2/2	80	54	30	16	SL	12.5	8.1	21.5	1.06	0.11	0.02
Profile 2 – *Spolic Technosol (Loamic, Eutric, Calcaric, Humic, Hyperartefactic, Skeletic, Toxic)* Approximate time of soil origin: late 18th c. – mid-19th c.													
Oi	0–1	–	–	–	–	–	–	–	–	–	43.97	0.98	0.07
AC1	1–25	10YR 2/2	40	75	19	6	SL	32.2	7.5	22.1	6.62	0.44	0.06
AC2	25–45	10YR 3/1	60	70	21	9	SL	33.7	7.9	21.2	2.63	0.17	0.03
AC3	45–65	10YR 3/2	70	65	23	12	SL	32.6	7.9	20.8	2.42	0.15	0.04
2C	65–90	2.5YR 3/2	80	46	40	14	L	22.4	7.8	9.6	2.70	0.24	0.04
Profile 3 – *Spolic Technosol (Epiarenic, Endoloamic, Eutric, Dolomitic, Mollic, Hyperartefactic, Skeletic)* Approximate time of soil origin: late 18th c. – 19th c.													
Oe	0–6	7.5YR 3/3	–	–	–	–	–	–	5.7	–	41.22	1.65	0.13
O/C	6–25	10YR 2/1	70	87	9	4	LS	32.3	6.8	11.1	23.57	1.11	0.12
AC	25–40	10YR 2/2	70	81	15	4	LS	15.1	7.2	17.0	10.69	0.53	0.07
BC	40–60	10YR 3/4	40	70	24	6	SL	6.5	7.6	26.5	5.14	0.26	0.04
Profile 4 – *Spolic Technosol (Epiarenic, Endoloamic, Eutric, Humic, Hyperartefactic)* Approximate time of soil origin: late 18th c. – early 19th c.													
Oi	0–1	–	–	–	–	–	–	–	–	–	–	–	–
A	1–13	10YR 2/2	50	85	11	4	LS	22.3	6.1	n	8.41	0.54	0.06
C1	13–35	7.5YR 5/4	30	58	25	17	SL	8.0	6.8	n	0.49	0.07	0.02
C2	35–60	10YR 5/4	30	57	25	18	SL	7.9	6.9	n	0.29	0.06	0.01
Profile 5 – *Spolic Technosol (Arenic, Epidystric, Endoeutric, Protocambic, Humic, Hyperartefactic, Skeletic, Toxic)* Approximate time of soil origin: 15th c. – late 19th c.													
Oe	0–3	10YR 2/2	–	–	–	–	–	–	4.1	–	44.95	2.06	0.15
Oa	3–10	10YR 2/1	–	–	–	–	–	–	3.7	–	23.09	1.20	0.12
A	10–15	10YR 2/1	50	86	11	3	LS	15.6	4.0	n	4.62	0.29	0.10
Bw	15–20	10YR 3/3	70	78	18	4	LS	13.4	4.4	n	1.79	0.14	0.09
C	20–45	10YR 4/2	90	77	19	4	LS	14.0	6.0	n	1.01	0.09	0.08
Profile 6 – *Spolic Technosol (Epiloamic, Endoarenic, Dystric, Protocambic, Humic, Hyperartefactic, Skeletic, Toxic)* Approximate time of soil origin: 15th c. – late 19th c.													
Oe	0–2	10YR 2/2	–	0	0	0	–	–	4.0	–	37.86	1.67	0.14
Oa	2–10	10YR 2/1	–	0	0	0	–	–	3.6	–	27.23	1.23	0.11
ABw	10–20	10YR 3/3, 4/3	50	76	16	8	SL	10.2	3.9	n	1.16	0.10	0.06
C	20–65	5YR 5/1	90	79	14	7	LS	10.8	5.5	n	0.63	0.07	0.16

Table 1 – continue

Horizon	Depth (cm)	Munsell colour (moist)*	Rock fragments (%)*	Percentage of fractions (mm)			Soil textural class (USDA)	Magnetic susceptibility (χ) ($\times 10^{-8} \cdot m^3 \cdot kg^{-1}$)	pH_{H2O}	eq. $CaCO_3$ (%)	TOC (%)	TN (%)	TS (%)
				2.0–0.05	0.05–0.002	< 0.002							
Profile 7 – *Spolic Technosol (Epiarenic, Endoloamic, Dystric, Humic, Hyperartefactic, Skeletic)* Approximate time of soil origin: 15th c. – late 19th c.													
Oe	0–2	–	–	–	–	–	–	–	3.7	–	40.47	1.54	0.13
AC	2–15	10YR 2/1	50	86	13	1	S	32.5	3.8	n	10.93	0.65	0.08
C	15–50	10YR 3/4	70	65	32	3	SL	15.3	4.6	n	1.96	0.15	0.02
Profile 8 – *Spolic Technosol (Arenic, Dystric, Humic, Hyperartefactic, Skeletic, Toxic)* Approximate time of soil origin: 15th c. – late 19th c.													
Oe	0–4	–	–	–	–	–	–	–	4.0	–	46.96	1.58	0.12
AC	4–15	10YR 2/2	40	81	18	1	LS	15.5	3.8	n	3.02	0.16	0.57
C1	15–35	10YR 2/2	70	81	16	3	LS	11.8	4.5	n	1.26	0.10	0.15
C2	35–55	10YR 3/4	80	79	18	3	LS	10.5	4.3	n	1.44	0.11	0.12
Profile 9 – *Coarsic Spolic Technosol (Arenic, Amphiloamic, Dystric, Ochric, Hyperartefactic, Skeletic, Toxic)* Approximate time of soil origin: 16th c. – 19th c.													
Oi	0–2	–	–	–	–	–	–	–	–	–	45.82	0.91	0.08
AC	2–10	10YR 3/2	80	79	15	6	LS	14.4	4.4	n	1.05	0.10	0.40
C1	10–40	10YR 4/2	90	76	16	8	SL	14.4	4.5	n	0.88	0.09	0.37
C2	40–80	10YR 4/2	90	79	15	6	LS	13.3	4.5	n	0.86	0.09	0.53
Profile 10 – *Coarsic Spolic Technosol (Loamic, Dystric, Humic, Hyperartefactic, Skeletic, Toxic)* Approximate time of soil origin: 16th c. – 19th c.													
Oi	0–1	–	–	–	–	–	–	–	–	–	47.90	0.90	0.07
AC	1–10	10YR 3/2	70	76	17	7	SL	39.0	4.4	n	1.48	0.10	0.07
C1	10–50	10YR 4/2	90	77	16	7	SL	14.8	4.4	n	1.16	0.09	0.07
C2	50–70	10YR 4/4	70	76	18	6	SL	15.2	4.5	n	1.42	0.12	0.06
Profile 11 – *Spolic Technosol (Epiarenic, Endoloamic, Eutric, Carbonic, Humic, Hyperartefactic, Pyric, Toxic)* Approximate time of soil origin: 18th c. – early 19th c.													
Oi	0–1	–	–	–	–	–	–	–	–	–	40.20	1.22	0.09
A	1–15	10YR 2/1	5	79	14	7	LS	3313.6	5.6	n	9.13	0.55	0.06
C1	15–30	10YR 2/2, 4/3	10	65	26	9	SL	3342.2	6.0	n	5.24	0.29	0.04
C2	30–45	10YR 2/1	15	67	27	6	SL	7064.4	6.2	n	8.84	0.28	0.04
C3	45–60	10YR 2/1	20	69	26	5	SL	10485.6	6.5	n	10.60	0.22	0.04
Profile 12 – *Spolic Technosol (Epiarenic, Endoloamic, Eutric, Carbonic, Humic, Hyperartefactic, Pyric, Toxic)* Approximate time of soil origin: 18th c. – early 19th c.													
Oi	0–1	–	–	–	–	–	–	–	–	–	–	–	–
A	1–20	10YR 2/1	20	76	19	5	LS	4683.8	5.8	n	8.04	0.42	0.05
C1	20–28	10YR 5/4	20	67	24	9	SL	489.4	6.1	n	2.55	0.21	0.10
2C	28–50	10YR 2/1	50	65	29	6	SL	9480.3	6.1	n	14.69	0.16	0.03
3C	50–60	5YR 4/4	40	70	23	7	SL	161.2	6.6	1.7	1.44	0.08	0.75
4C	60–75	10YR 4/3	30	61	29	10	SL	36.6	6.4	n	1.87	0.18	0.05
Profile 13 – *Spolic Technosol (Arenic, Eutric, Humic, Hyperartefactic, Relocatic, Skeletic)* Approximate time of soil origin: late 18th c. – late 19th c.													
Oi	0–1	–	–	–	–	–	–	–	–	–	45.07	1.18	0.07
AC	1–15	10YR 2/1	80	80	18	2	LS	128.0	7.0	1.3	6.03	0.38	0.10
2C	15–25	10YR 5/3	50	84	11	5	LS	28.3	8.6	5.8	5.63	0.38	0.10

Explanations: – not analysed; n – not detected; * measured during field works; L – loam; LS – loamy sand; S – sand; SL – sandy loam; TOC – total organic carbon; TN – total nitrogen; TS – total sulphur.

2.3.3. SEM-EDS analyses

The selected soil thin sections were studied using a scanning electron microscope equipped with an energy dispersive X-ray spectrometer (SEM-EDS). The samples were carbon-coated before the analyses in SEM-EDS. The SIGMA (Zeiss) field emission SEM was used. The microscope was equipped with the backscattered electron (BSE) detector. The studies were performed in a high vacuum mode using an accelerating voltage of 20 kV. The analyses were performed at the Laboratory of Electron Microscopy, Microanalysis, and X-Ray Diffraction, Faculty of Geology, University of Warsaw, Poland.

2.3.4. Pedogenic forms of Fe, Al, Si, and Mn

The selective extractions of pedogenic Fe, Al, Si, and Mn forms were performed on soil fine earth (<2 mm). The analyses included the following extractions:

- dithionite–citrate–bicarbonate (DCB) Fe extraction; it was used to extract free iron oxides (denoted hereafter as Fe_d), following the procedure by Mehra and Jackson (1958),
- ammonium oxalate extraction using a solution of 0.175 M ammonium oxalate and 0.1 M oxalic acid (at pH 3.0) in the darkness; it was applied to extract amorphous and poorly crystalline forms of Fe, Al, Si, and Mn (denoted hereafter as Fe_{ox}, Al_{ox}, Si_{ox}, and Mn_{ox}), according to the method by Schwertmann (1964).

The Fe, Al, Si, and Mn concentrations in the soil extracts were measured using inductively coupled plasma – optical emission spectrometry (ICP–OES, Perkin Elmer Avio 200). The total iron content (Fe_t) was determined on powdered soil fine earth by total microwave mineralisation (Milestone Ethos UP) in a mixture of concentrated acids (2 ml HNO_3 + 5 ml HF + 2 ml HCl + 1 ml $HClO_4$) and analysis of extracts using ICP-OES. All analyses were performed in duplicates.

Based on the measured forms (Fe_t, Fe_d, Fe_{ox}, Al_{ox}), the following parameters were calculated:

- Fe_{nf} – iron content in forms other than free oxides, calculated as $Fe_{nf} = Fe_t - Fe_d$
- Fe_c – crystalline pedogenic iron oxides, calculated as $Fe_c = Fe_d - Fe_{ox}$
- Fe_d/Fe_t – Fe oxide mobility index
- Fe_{ox}/Fe_d – Fe oxide activity index
- Al_{ox} + ½Fe_{ox} (expressed in %), which is used as one of the indicators of the spodic horizon according to the WRB soil classification system (IUSS Working Group WRB, 2022).

3. Results

3.1. Morphology, properties, and mineral composition of the studied Technosols

Detailed information about properties, mineral and chemical composition, as well as photographs of soil profiles and the surrounding vegetation, was presented elsewhere (Tarnawczyk et al., 2024, 2025). Selected physical and chemical properties are presented in Table 1. Profiles 1–10 represented soils developed from mine waste dumps containing diverse parent materials including limestone and dolomite debris, granite and gneiss fragments. Most profiles showed a simple soil morphology consisting of O, A (or AC) and C horizons, except for profiles 5 and 6, which had Bw horizons suggesting more advanced soil-forming processes. A high content of rock fragments was a common feature of most of the studied profiles. Profiles 11–13 represented Technosols formed in areas of old metallurgical activity. Profiles 11 and 12, near the Stare Kościeliska steelworks, contained slag, ferruginous rocks, charcoals, and building debris. Profile 12 displayed clear layering and contained layers rich in both metallurgical wastes (A and 2C horizons) and mine wastes (3C horizon). Profile 13, at an artificial slag disposal site in Kuźnice, was composed of carbonate-bearing sandy material covered with slag fragments, forming a thin, bipartite soil profile.

Technosols developed from carbonate-rich mine wastes (group I) were characterised by neutral to alkaline reaction (pH from 7.2 to 8.1, except for horizon Oe and O/C in P3 with pH 5.7 and 6.8, respectively), resulting from the high carbonate content (9.6–31.2% $CaCO_3$ eq.) (Table 1) (Tarnawczyk et al., 2024). They exhibited moderate to high concentrations of total organic carbon (TOC) in organic horizons (43% on average; 24% in horizon O/C, P3), with lower values in the mineral horizons (4% on average). These soils contained a high proportion of rock fragments (up to 80%), and the soil texture of the fine earth was sandy loam, loamy sand, or loam. Magnetic susceptibility values varied from 7 to 91 $\times 10^{-8} \cdot m^3 \cdot kg^{-1}$. Mineral composition, as previously determined by X-ray diffraction (XRD) (Tarnawczyk et al., 2024) included calcite, quartz, dolomite, feldspars, hematite, and clay minerals.

Technosols developed from non-carbonate aluminosilicate mine wastes (group II) were acidic (pH 3.8–6.0 in mineral horizons; pH 3.9 in organic horizons, on average) (Table 1) due to the absence of carbonates and the weathering of igneous and metamorphic rocks such as granite and gneiss under a coniferous forest vegetation (Tarnawczyk et al., 2024). The TOC contents were generally lower than in group I (2% on average), with higher values obtained in organic (O) horizons (39% on average). The content of rock fragments often exceeded 70% and the soil texture of the fine earth was dominantly loamy sand. Magnetic susceptibility values were from 10 to 39 $\times 10^{-8} \cdot m^3 \cdot kg^{-1}$. Common minerals included quartz, feldspars, and micas, with occasional presence of jarosite and pyrite.

Technosols containing metallurgical wastes (group III) showed variable reaction from slightly acidic to strongly alkaline (pH from 5.6 to 8.6) (Table 1) (Tarnawczyk et al., 2024). The TOC concentrations were notably higher than in the mining non-carbonate waste soils (7% on average in mineral horizons, 43% on average in organic horizons), with high TOC concentrations in horizons enriched in charcoal (up to 15% horizon 2C in P12). Magnetic susceptibility was exceptionally high (up to 10486 $\times 10^{-8} \cdot m^3 \cdot kg^{-1}$) reflecting the presence of magnetic minerals such as magnetite and wüstite. These soils also contained fayalite, goethite, as well as alumino-silicate and ferrous slag residues.

3.2. Soil micromorphological features

3.2.1. Technosols developed from mine wastes containing carbonate-bearing rocks (group I)

Technosols of group I (profiles 1–3) were composed of carbonate sedimentary rock (limestones, dolomites) fragments with

admixture of siliceous sedimentary rocks and fine soil material occurring between rock fragments (Fig. 1A–F, Table 2). Soil material was characterised by a highly separated complex (intergrain micro-aggregate) microstructure with complex, compound, and simple packing voids, as it was found, e.g., in profile 2, AC1 horizon and profile 1, the transition between C and 2C horizons (Fig. 1 C–F).

The groundmass occurred as crumbs or subangular blocky aggregates with porphyric c/f related distribution (Fig. 1A and B; Table 2). Fragments of carbonate, Fe-bearing, and siliceous rocks, as well as separate carbonate, quartz, and feldspar grains, represented coarse fragments in the aggregates. Iron oxide pseudomorphs after sulphides were identified in the transition between C and 2C horizons in profile 1 (Fig. 1E and F; Fig. 2A). Micromass of topsoil horizons was a dark brown or dark grey material with an undifferentiated b-fabric. Micromass of subsoil horizons was a red or red-brown material with an undifferentiated b-fabric. Roots were occasionally found throughout the soil thin sections.

Few pedofeatures were observed under the optical microscope. Occasional carbonate coatings on ped faces and void walls were found, e.g. in the transition between C and 2C horizons in profile 1 (Fig. 1G and H). These coatings exhibited low birefringence and appeared limpid under crossed polarisers.

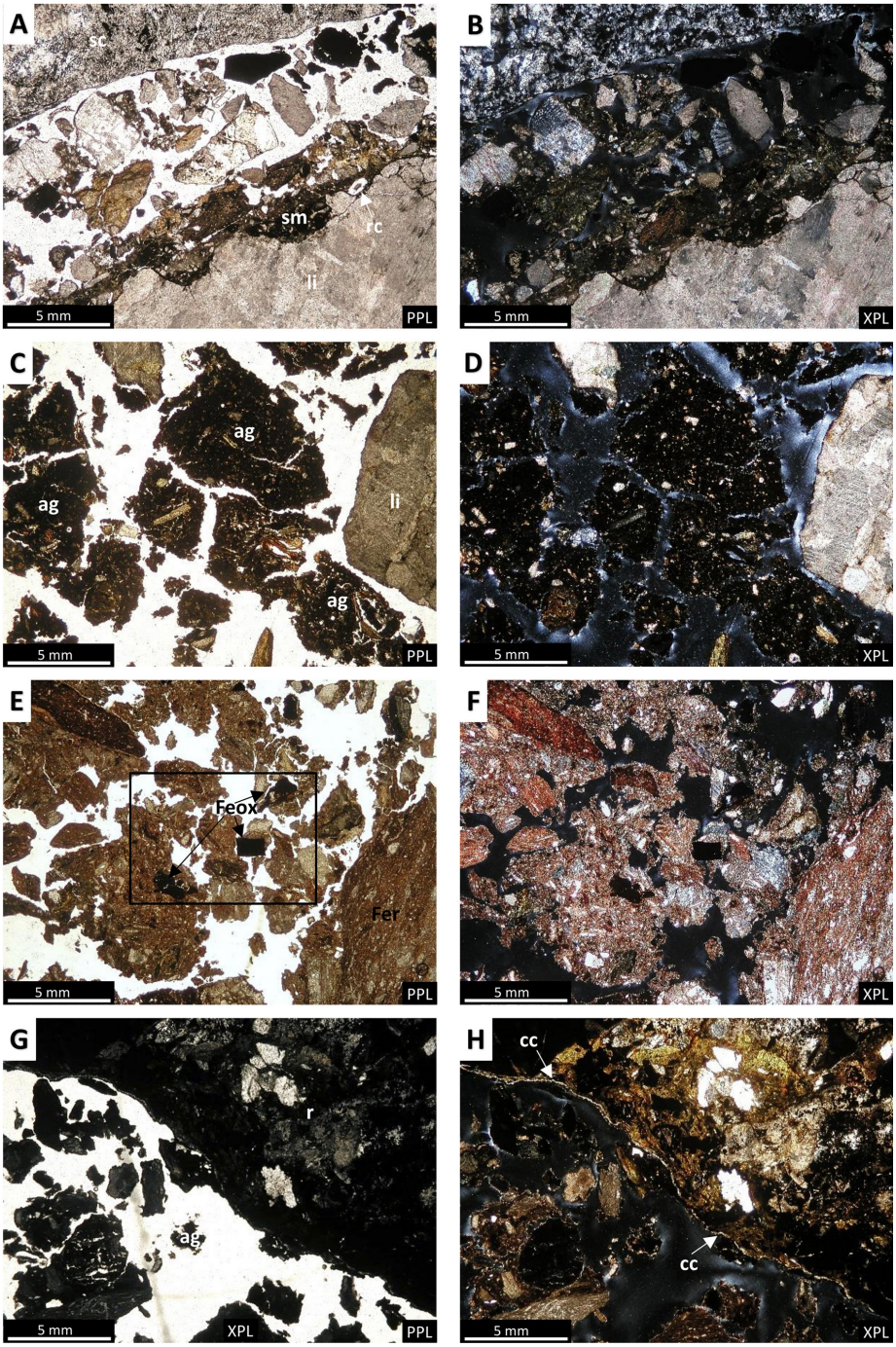

Fig. 1. Micromorphological features of Technosols developed from mine wastes comprising carbonate rocks (group I). **A and B** – profile 1, AC2 horizon. A channel between a limestone (li) and a siliceous rock (sc) filled with rock and mineral fragments. Dark brown soil micromass (sm) rich in humus occurs on a limestone fragment. Root channel (rc) occurs in the micromass. **C and D** – profile 2, AC1 horizon. Limestones (li) and soil aggregates (ag) composed of humic substances and coarse components, including carbonate grains and ferruginous rocks. **E and F** – profile 1, the transition between C and 2C horizons. A groundmass composed of Fe-bearing rocks (Fer), limestone fragments, Fe oxide (Feox) fragments, and a micromass containing clay minerals and dispersed Fe oxides (most likely hematite). A fragment in the framework is shown in detail in Fig. 2A. **G and H** – profile 1, the transition between C and 2C horizons. A carbonate coating (cc) along the pore surrounded by soil aggregates (ag) and a complex sedimentary rock fragment (r) composed, among others, of carbonates and Fe- and Mn-bearing ore minerals. Explanations: PPL – plane-polarized light, XPL – crossed polarizers

Table 2
Micromorphological features of Technosols based on thin sections from selected soil horizons

Profile	Horizon	Depth (cm)	Microstructure	Voids	Rock fragments	Groundmass			Organic matter	Pedofeatures	Other features
						The c/f related distribution	Coarse mineral material	Micromass (fine material): shape, colour, b-fabric			
P1	AC2	5–15	C	SPV	CSR, SiR, FeR	P	C, Qz, Feox, Mnox, Fsp	RBr, G, un	COR, PR	–	PS, MD
P1	transition between C and 2C	~35	C (G, IMA)	SPV, CPV	CSR, SiR, FeR	P	C, Qz, Feox, Mnox, Fsp, Mca	SAB, R, RBr, G, un	C, COR	SCCC	PS, SOM
P2	AC1	1–25	IMA	CXV	CSR, SiR, FeR	P	C, Qz, Feox, Mnox, Fsp, Mca	CA, SAB, RBr, G, un	PR, Ch	–	AS, MV, PS
P4	C1	13–35	S	CXV, PV	IR, MR	–	C, Qz, Fsp, Mca	YRBr, G, un	PR	–	–
P5	transition between A and Bw	~15	SG	SPV	IR, MR	coarse M	Qz, Feox, Fsp, Mca, Chl	RBr, YRBr, un	–	ICC	PS
P6	ABw	10–20	SG	SPV	IR, MR	coarse M	Qz, Feox, Fsp, Mca	RBr, YRBr, un, grs	PR	ICC	PS
P8	transition between AC and C1	~15	C	CXV	IR, MR	–	Qz, Feox, Fsp, Mca, Chl, Brt	G, YBr, un	–	MnC	–
P8	transition between AC and C1	~15	C	CXV	IR, MR	–	Qz, Feox, Fsp, Mca, Chl	G, YBr, un	–	–	BP, AS, WRM
P9	AC	2–10	SG	SPV	IR, MR	–	Qz, Feox, Fsp, Mca	RBr, YRBr, un	PR	ICC	PS, AS
P10	AC and C1	~10	C	CXV	IR, MR	–	Qz, Feox, Fsp, Mca	YBr, G, un	–	–	–
P10	C2	50–70	C	CXV	IR, MR	–	Qz, Feox, Fsp, Mca	YBr, G, un	–	–	–
P11	transition between A and C1	~10	C	CXV	SL, NSR	–	Qz, Feox, Fsp, Mca	CA, Bl, un	Ch	ICC	SO
P11	C2	30–45	C	CXV	SL, NSR	–	Qz, Feox, Fsp, Mca	CA, Bl, un	Ch	ICC	–
P12	A	1–20	C	CXV	SL, NSR	–	Qz, Feox, Fsp, Mca	CA, Bl, un	Ch	ICC	–
P12	2C	28–50	C	CXV	SL, NSR	–	Qz, Feox, Fsp, Mca	CA, Bl, un	Ch	ICC around charcoal	–
P13	AC	1–15	C	CXV	SL	–	Qz	Br, un	–	–	–

Explanations:
– not determined
Microstructure: C – complex microstructure, G – granular microstructure, IMA – intergrain micro-aggregate microstructure, S – subangular blocky microstructure, SG – single grain microstructure
Voids: CPV - compound packing voids, CXV – complex packing voids, PV – planar voids, SPV – simple packing voids
Rock fragments: CSR – carbonate sedimentary rocks (limestones, dolomites), IR – igneous rocks (granite), MR – metamorphic rocks (gneiss), NSR – non-carbonate sedimentary rocks (sandstones, mudstones), SiR – siliceous sedimentary rocks, FeR – Fe-bearing rocks, SL – slags
The c/f related distribution: E – enaulic, M – monic, P – porphyric
Coarse mineral material: Brt – barite, C – carbonates, Chl – chlorite, Fsp – feldspar, Feox – iron oxides, Mnox – manganese oxides, Mca – mica, Qz – quartz
Micromass (fine material): Bl – black, Br – brown, CA – crumb aggregates, G – grey, grs – granostriated b-fabric, R – red, RBr – reddish-brown, SAB – sub-angular blocks, un – undifferentiated b-fabric, YBr – yellowish brown, YRBr – yellowish reddish-brown
Organic matter: Ch – charcoal, COR – carbonate organic remains (in rocks), PR – plant residues
Pedofeatures: BP – biotic pedoturbations (chanells), ICC – Fe oxide coatings, SCCC – secondary Ca carbonates coating, MnC – Mn oxide coatings
Other features: MV – Mn oxide veins (in rocks), MD – Mn oxide dendrites, PS – Fe oxide pseudomorphs after sulphides, SOM – soil organic matter, AS – aggregate structure, WRM – strongly weathered rocks and mineral fragments, SO – soil organisms

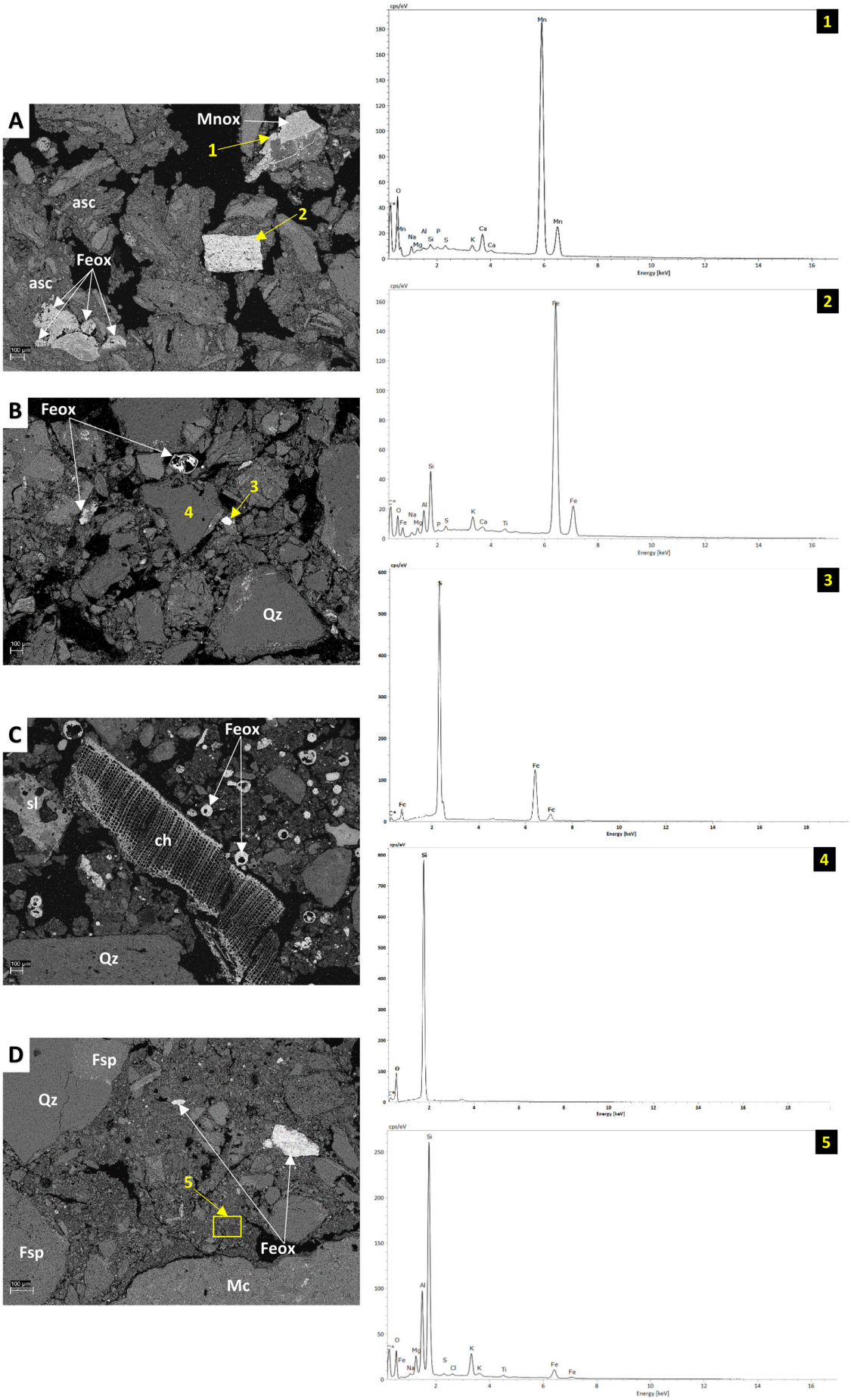

Fig. 2. Soil groundmass features in back-scattered electron (BSE) images and the EDS spectra for selected points or microareas. **A** – profile 1, the transition between C and 2C horizons. The groundmass containing limestone fragments, micromass consisting of aluminosilicate clays (asc) and Fe oxides, Mn oxides (Mnox), and pseudomorphs of Fe oxides (Feox) after sulphides. Voids are black. **B** – profile 6, ABw horizon. Groundmass consisting of quartz (Qz), aluminosilicates (e.g. feldspars), and pseudomorphs of Fe oxides (Feox) after sulphides. Voids are black. **C** – profile 11, the transition between A and C1 horizons. Charcoal (ch) and the groundmass containing slag (sl), quartz (Qz), spherical grains of Fe oxides (Feox) (most likely magnetite), and the micromass rich in clays and humic substances. Voids are black. **D** – profile 4, C1 horizon. Groundmass consisting of quartz (Qz), feldspars (Fsp), micas (Mc), and the micromass with a considerable share of clay minerals. Voids are black

3.2.2. Technosols developed from mine wastes containing granite and gneiss (group II)

Technosols of group II (profiles 5–10) originated from mine wastes comprising igneous (granite) and metamorphic (gneiss) rock fragments. A complex microstructure was dominant in the soils, interspersed with granular aggregates (Fig. 3 A–J) (Table 2). Complex packing voids and simple packing voids occurred between coarse fragments and soil aggregates.

The groundmass had coarse monic c/f related distribution (Table 2). It was composed of soil microaggregates and poorly weathered rock and mineral fragments (Fig. 3G and H). The predominant mineral grains were quartz, muscovite, biotite, fine-grain mica (sericite), chlorite, and Fe oxides (Fig. 3I and J) (Table 2). Fe sulphides were rarely found (Fig. 2B). The micromass was composed most likely of clay minerals and Fe oxides, and it had a yellowish brown colour, as well as undifferentiated and granostriated b-fabric as it was found in ABw horizon in profile 6 (Fig. 3C and D). Well-developed crumb-like aggregates predominated (Fig. 3E and F). Occasional Fe oxide-bearing coatings on rock fragments were observed as it was identified in the transition between A and Bw horizons in profile 5 (Fig. 3A and B). Moreover, bioturbations in the form of channels filled with soil material that was most likely reworked by soil fauna were also found, e.g., in the transition between AC and C1 horizons in profile 8 (Fig. 3G and H).

3.2.3. Technosols containing metallurgical wastes (group III)

Technosols of group III (profiles 11–13) contained metallurgical wastes including slags, as the major soil substrate. The microstructure of these soils was complex with weak granular microaggregates (Fig. 4 A–J) (Table 2). Complex packing voids were present between coarse fragments and soil aggregates.

The groundmass was composed mainly of metallurgical slag fragments with hollows often inhabited by soil organisms (most likely some nematode or enchytraeid) and filled with a soil micromass reworked by these animals, well visible in the transition between A and C1 horizons in profile 11 (Fig. 4A and B). Slags were composed of pyroxene and magnetite (Fig. 4G and H), but some of them were amorphous materials (Fig. 4I and J) (Table 2). Common coarse components in the groundmass were spherical iron oxides, most likely magnetite (Fig. 2C). Micromass was dark brown and black as it contained an admixture of organic carbon. Dark soil colour was related to the abundance of charcoal fragments, noted e.g. in profile 11, the transition between A and C1 horizon (Fig. 2C), and organic matter of anthropogenic origin dispersed in the micromass. Transformed plant residues were occasionally found in the soils. Brownish aggregates composed of allochthonous clay mineral-bearing soil material were found in profile 11, C2 horizon, and in profile 12, A horizon (Fig. 4C–F). These aggregates most likely originated from mixing local native soil with anthropogenic material formed during smelting activity.

3.2.4. Technosols developed from mine wastes having the features of group I and II soils

Parent material of profile 4 was a mixture of carbonate sedimentary rocks, igneous, and metamorphic rocks. The soil substrate was characterised by subangular blocky microstructure (Fig. 5 A–D) (Table 2). Complex packing voids and smooth planar voids were the most common void types.

The groundmass showed two types of soil micromass: yellowish brown and reddish brown. Groundmass had porphyric c/f related distribution and undifferentiated b-fabric (Fig. 5 A–D). It consisted of aluminosilicate clays with an admixture of Fe oxides (Fig. 2D). Coarse material was represented by fragments of quartz, feldspars, carbonates, micas (Fig. 5A and B; Table 2), and Fe oxides (Fig. 2D). Organic matter consisted of dark brown organic residues dispersed in micromass and channels. Channels were often filled with roots (Fig. 5C and D).

3.3. SEM-EDS analyses

Detailed examination of soil material in group I revealed the presence of a pseudomorph of Fe oxides after sulphides in the transition between C and 2C horizons in profile 1 (Fig. 6). This pseudomorph was composed entirely of Fe oxides. Based on the crystal habit, it can be supposed that this pseudomorph was formed due to the weathering of primary Fe sulphides. The pseudomorph was surrounded by rock fragments composed of aluminosilicates (feldspars, micas). Fragments of carbonate minerals were dispersed in the soil micromass composed of aluminosilicate clays and Fe oxides. Moreover, a coating of secondary Ca carbonates was found on the surface of a feldspar grain (Fig. 6).

SEM-EDS analyses of a groundmass in profile 8 (the transition between AC and C1 horizons), representing group II Technosols, showed that rock fragments were composed of aluminosilicates, quartz, and Fe oxides (Fig. 7). The groundmass contained coarse components: aluminosilicates (feldspars, micas, chlorite), quartz, and barite. The peaks of Ti–Kα (4.51 keV) and Ba–Lα (4.47 keV) in the EDS spectra partially overlapped; however, careful comparison of EDS maps for Ti and Ba enabled a clear distinction between Ba-bearing and Ti-bearing phases (Ti-bearing minerals in the soil groundmass are indicated by the red colour in the EDS map for Ti) (Fig. 7). Soil micromass was composed of aluminosilicate clays. The map for Mn revealed the occurrence of coatings composed of Mn-bearing phases (most likely Mn oxides). The coatings occurred on both rock fragments and seem to be pedogenic in origin.

The soil material in profile 11 (the transition between A and C1 horizons) representing group III is presented in Fig. 8. It was composed of slag and quartz fragments and the groundmass between these fragments. The slag consisted mainly of Fe, Al, K, and Ca, and contained acicular Fe-bearing phases (most likely Fe oxides). The groundmass contained quartz, aluminosilicates (most likely feldspars and micas), and Fe oxide spherules as coarse components. The micromass was likely composed of aluminosilicate clays, but also contained a remarkable contribution of S and P, suggesting the occurrence of organic compounds. The elemental map for S (Fig. 8) revealed the presence of a coating containing S-bearing compounds, most likely some sulphates.

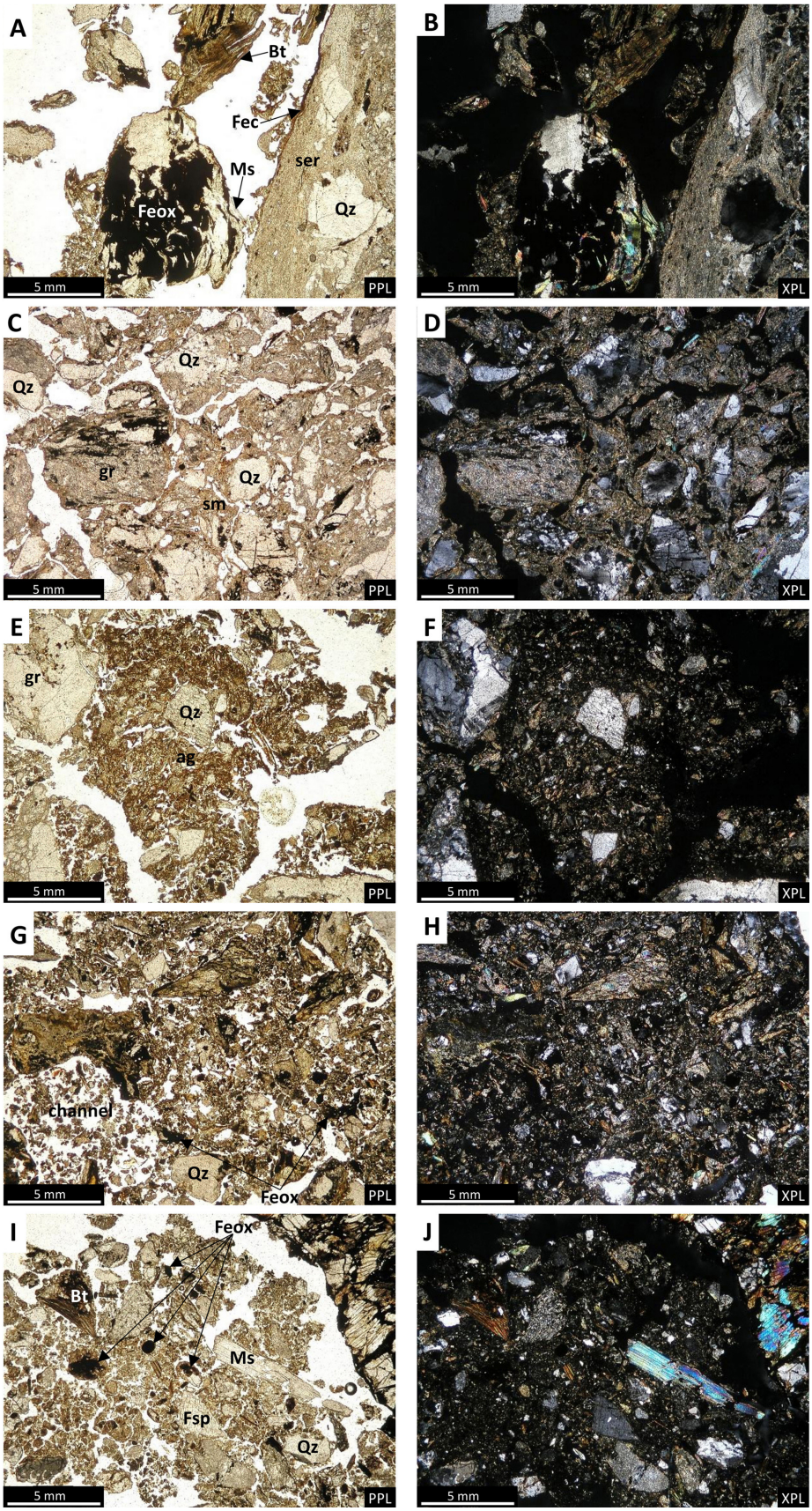

Fig. 3. Micromorphological features of Technosols developed from mine wastes comprising igneous and metamorphic rocks (granite and gneiss) (group II). **A and B** – profile 5, transition between A and Bw horizons. Rock fragments composed of quartz (Qz), muscovite (Ms), biotite (Bt), fine-grain mica (sericite) (ser), and Fe oxides (Feox), accompanied by soil material. Note the occurrence of a Fe oxide-bearing coating (Fec) on a rock fragment. **C and D** – profile 6, ABw horizon. The granite (gr) fragment, quartz grains (Qz), and the soil micromass (sm) composed of clay minerals and Fe oxides exhibiting granostriated b-fabric and surrounding rock fragments and mineral grains. **E and F** – profile 6, ABw horizon. Brown soil aggregate (ag) composed of micromass containing clay minerals and Fe oxides, as well as granite fragments (gr) and quartz (Qz) grains. **G and H** – profile 8, the transition between AC and C1 horizons. Groundmass composed of soil microaggregates and poorly weathered rock and mineral fragments (quartz – Qz, Fe oxides – Feox). Note the occurrence of a channel (bottom left) filled with soil material that is most likely reworked by soil fauna. **I and J** – profile 9, AC horizon. A groundmass consisting of feldspars (Fsp), quartz (Qz), muscovite (Ms), biotite (Bt), Fe oxides (Feox) as well as brown soil micromass characterized by undifferentiated b-fabric and composed of clay minerals and Fe oxides. Explanations: PPL – plane-polarized light, XPL – crossed polarizers

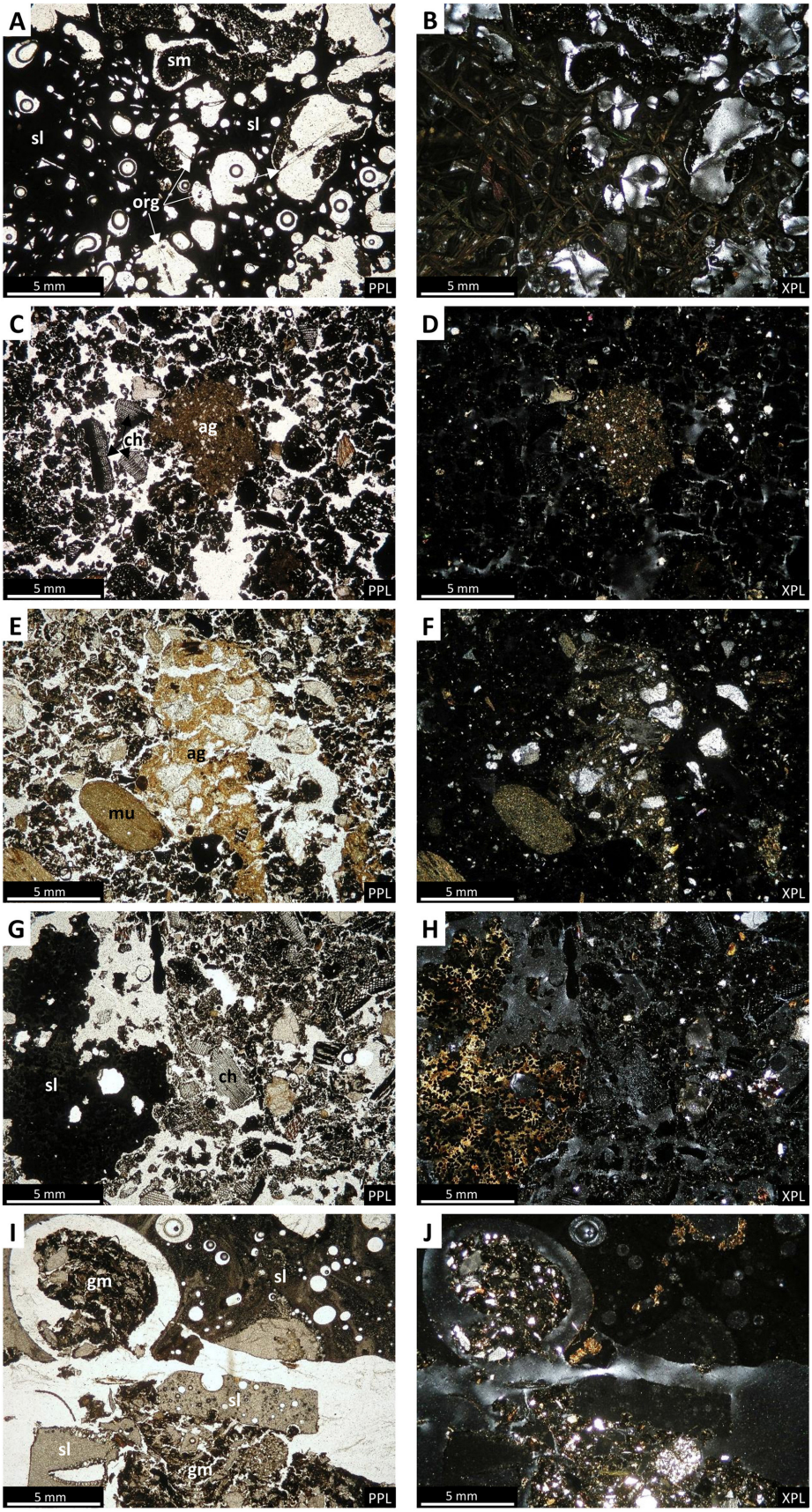

Fig. 4. Micromorphological features of Technosols developed in historical smelting areas (group III). **A and B** – profile 11, the transition between A and C1 horizons. A black metallurgical slag (sl) fragment with hollows partly inhabited by elongated tubular soil organisms (most likely some Nematoda or Enchytraeidae) (org); hollows are filled with a soil micromass (sm) reworked by these animals. **C and D** – profile 11, C2 horizon. Brownish aggregate (ag) composed of soil material surrounded by a dark material containing charcoals (ch) and the organic matter of anthropogenic origin. Brownish aggregate most likely originated from mixing local soil with anthropogenic material formed during smelting activity. **E and F** – profile 12, A horizon. Brownish aggregate (ag) composed of soil material and rounded mudstone (mu) fragment surrounded by a dark material containing organic matter of anthropogenic origin. Brownish aggregate most likely originated from mixing local soil with anthropogenic material formed during smelting activity. **G and H** – profile 12, 2C horizon. A slag (sl) fragment composed of pyroxene and magnetite, charcoals (ch), and a dark material rich in organic matter of anthropogenic origin. **I and J** – profile 13, AC horizon. Slag (sl) fragments and the groundmass (gm) being a mixture of dark organic matter, rock fragments, and mineral grains. Explanations: PPL – plane-polarized light, XPL – crossed polarizers

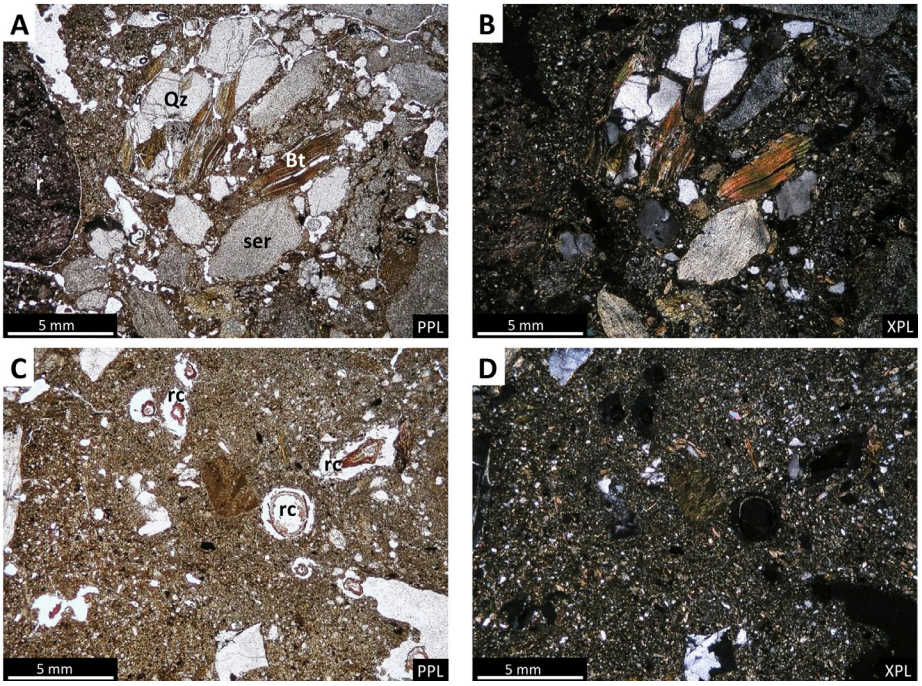

Fig. 5. Micromorphological features of Technosol having features of group I and II (profile 4). **A and B** – C1 horizon. Two types of soil micromass with Fe oxides surrounding different rock (r) fragments and mineral grains, e.g. quartz (Qz), biotite (Bt), and fine-grain mica (sericite) (ser). **C and D** – C1 horizon. Soil micromass consisting of clay minerals and Fe oxides having root channels (rc) filled with plant tissues. Explanations: PPL – plane-polarized light, XPL – crossed polarizers

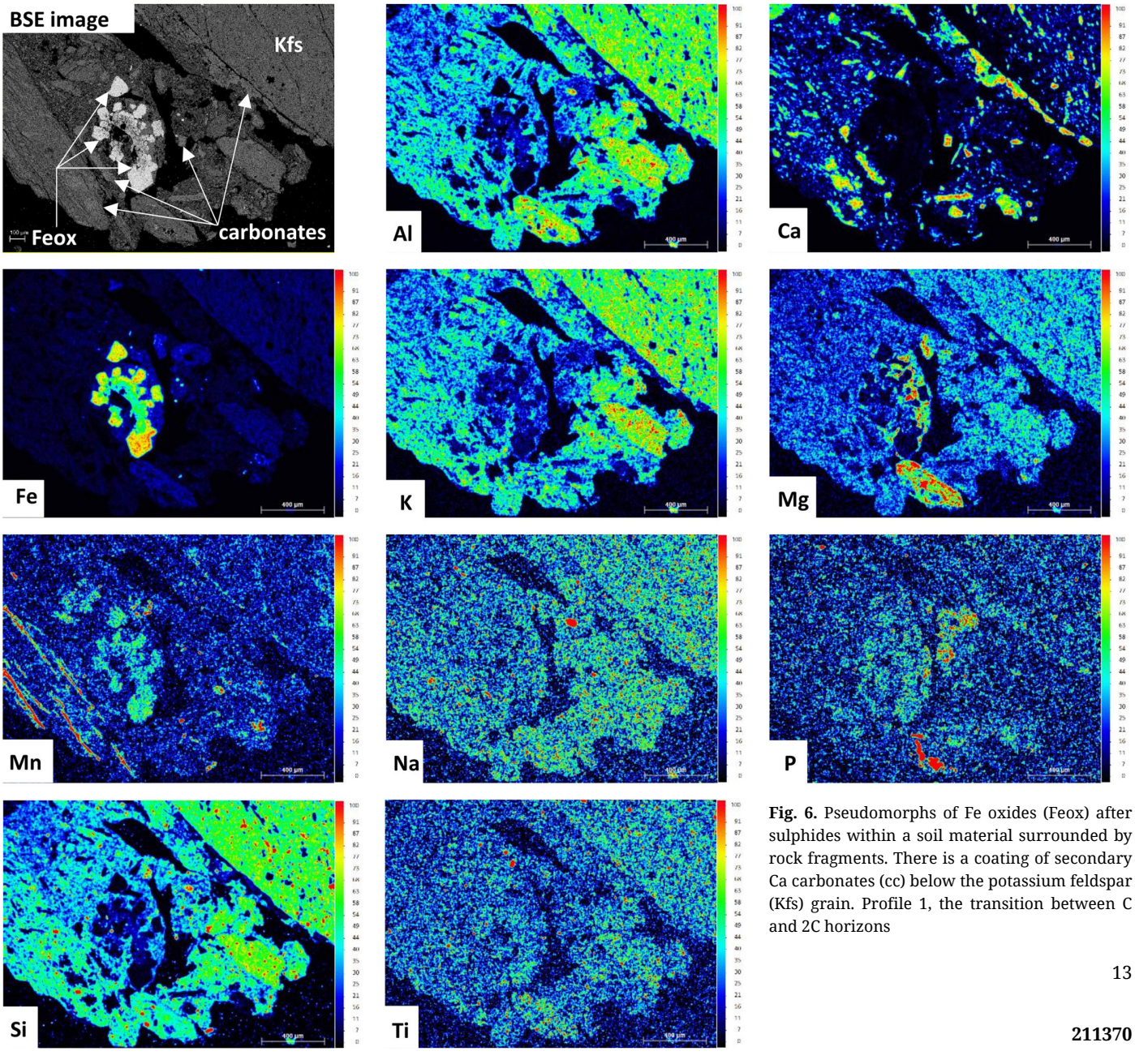

Fig. 6. Pseudomorphs of Fe oxides (Feox) after sulphides within a soil material surrounded by rock fragments. There is a coating of secondary Ca carbonates (cc) below the potassium feldspar (Kfs) grain. Profile 1, the transition between C and 2C horizons

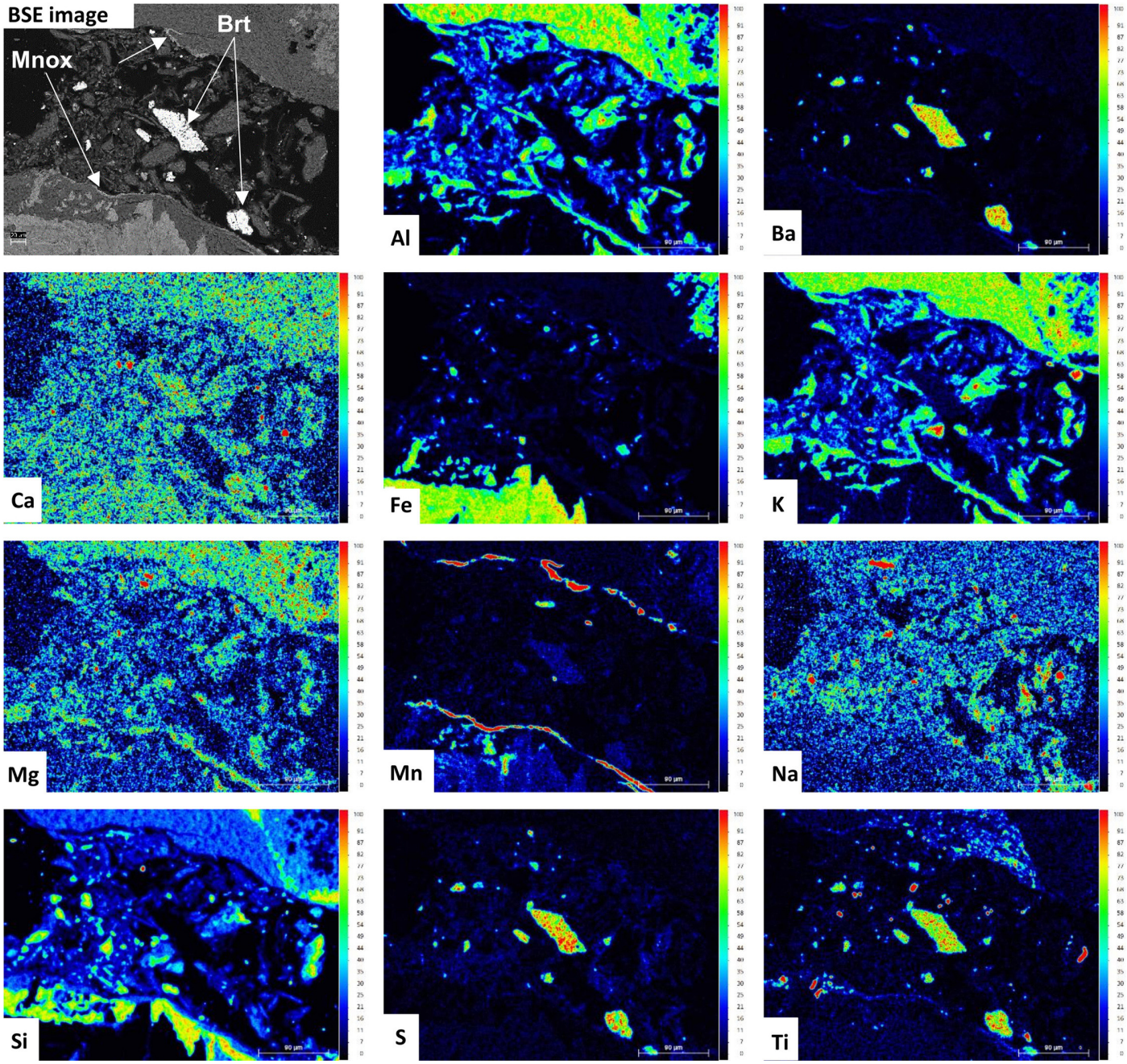

Fig. 7. A space between two rock fragments filled with fine grains of aluminosilicates and barite (Brt). Surfaces of rock fragments are covered with coatings composed of Mn oxides (Mnox). Profile 8, the transition between AC and C1 horizons

3.4. Pedogenic forms of Fe, Al, Si, and Mn

The Fe_t contents ranged from 7484 to 344307 mg·kg^{-1}, Fe_d from 1273 to 50639 mg·kg^{-1} and Fe_{ox} from 499 to 93449 mg·kg^{-1} across all profiles (Table 3). The analysis of pedogenic forms revealed distinct differences in the Fe_d/Fe_t and Fe_{ox}/Fe_d ratios across the studied profiles. In profiles 1 to 3 representing soils derived from carbonate rock mine wastes (group I), the Fe_d/Fe_t and the Fe_{ox}/Fe_d ratios averaged 0.38 and 0.22, respectively. Profile 3 showed clearly higher Fe_{ox}/Fe_d values (0.53 on average), indicating distinct chemical characteristics or more advanced effects of the soil-forming process in profile 3. In profiles 5 to 10 representing soils derived from aluminosilicate igneous and metamorphic rock mine waste (group II), the Fe_d/Fe_t and Fe_{ox}/Fe_d ratios averaged 0.32 (Table 3). The content of Fe_{ox} averaged 3531 mg·kg^{-1} and the content of Fe_d averaged 13519 mg·kg^{-1} in these profiles. In profile 4 having characteristics of groups I and II, the Fe_d/Fe_t ratio and the Fe_{ox}/Fe_d ratio averaged 0.41 and 0.18, respectively. Profiles 11 and 12 representing soils containing metallurgical wastes (group III), showed exceptionally high Fe_t content (192591 mg·kg^{-1} on average) (Table 3). The Fe_d/Fe_t ratio averaged 0.25 in profiles 11 and 12. Moreover, the content of Fe_{ox}

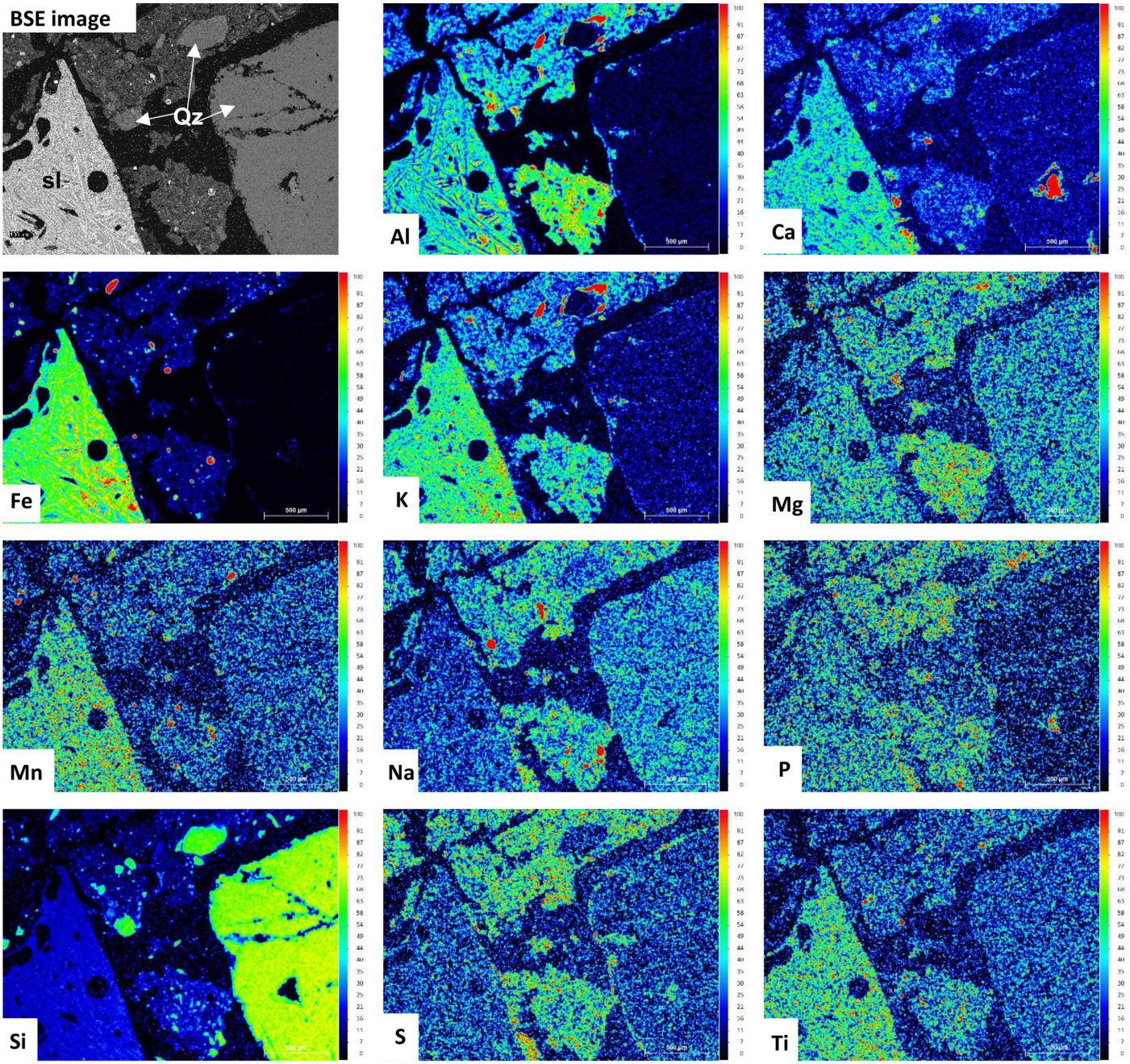

Fig. 8. A slag (sl) fragment composed mainly of Fe, K, Al, Ca, Mn, Ti, and the quartz (Qz) grain surrounded by the groundmass containing mainly Al, K, Mg, Na, S, and P. Note the occurrence of a coating containing S around the quartz grain. Profile 11, the transition between the A and C1 horizons

(57452 mg·kg^{-1} on average) was higher than the concentrations of Fe_d (39388 mg·kg^{-1} on average) in these profiles. Consequently, the Fe_{ox}/Fe_d ratio was high in profiles 11 and 12 (1.40 on average). Profile 13, also representing group III, exhibited a lower Fe_d/Fe_t ratio, averaging 0.16, with Fe_{ox}/Fe_d ratio averaging 0.64 (Table 3).

The Al_{ox}, Si_{ox}, and Mn_{ox} concentrations varied across the profiles (Table 3). In group I (profiles 1–3), Al_{ox} values averaged 1578 mg·kg^{-1}, Si_{ox} 225 mg·kg^{-1}, and Mn_{ox} 17699 mg·kg^{-1}. In group II, Al_{ox}, Si_{ox}, and Mn_{ox} contents averaged 1747, 156, and 2136 mg·kg^{-1}, respectively. Profile 4 exhibited the following mean values for Al_{ox} (1018 mg·kg^{-1} on average), Si_{ox} (147 mg·kg^{-1} on average), and Mn_{ox} (563 mg·kg^{-1} on average). In group III, Al_{ox} content averaged 3298 mg·kg^{-1}, Si_{ox} 3565 mg·kg^{-1}, and Mn_{ox} 3758 mg·kg^{-1} (Table 3).

The content and distribution of Al_{ox} + ½Fe_{ox} varied across the profiles (Table 3). In group I (profiles 1–3), Al_{ox} + ½Fe_{ox} values were generally low, averaging 0.23%. In group II (profiles 5–10), Al_{ox} + ½Fe_{ox} values averaged 0.35%, while among profiles 5 and 6, the highest values occurred in Bw and ABw horizons. In group III (profiles 11–13), Al_{ox} + ½Fe_{ox} exhibited the highest values, averaging 2.70%. Profile 4 demonstrated a relatively low Al_{ox} + ½Fe_{ox}, averaging 0.20% (Table 3).

Table 3
Forms of Fe, Al, Si, and Mn in the studied Technosols

Profile	Horizon	Depth	Fe_t	Fe_d	Fe_{ox}	Al_{ox}	Si_{ox}	Mn_{ox}	$Fe_t - Fe_d$	$Fe_d - Fe_{ox}$	Fe_d/Fe_t	Fe_{ox}/Fe_d	$Al_{ox} + ½Fe_{ox}$
			$mg \cdot kg^{-1}$										(%)
Profile 1	Oi	0–1	–	–	–	–	–	–	–	–	–	–	–
	AC1	1–5	32168	11840	1076	1182	241	30043	20328	10764	0.37	0.09	0.17
	AC2	5–15	32290	10957	758	928	188	31838	21333	10199	0.34	0.07	0.13
	C	15–35	32933	19117	632	761	236	28362	13817	18484	0.58	0.03	0.11
	2C	35–60	43989	12140	804	783	255	4510	31849	11336	0.28	0.07	0.12
Profile 2	Oi	0–1	–	–	–	–	–	–	–	–	–	–	–
	AC1	1–25	32543	13169	884	1109	273	26917	19374	12285	0.40	0.07	0.16
	AC2	25–45	51424	14065	764	1031	300	28831	37360	13301	0.27	0.05	0.14
	AC3	45–65	47192	14539	877	1105	301	29762	32653	13662	0.31	0.06	0.15
	2C	65–90	48343	12201	4963	3289	447	13915	36142	7238	0.25	0.41	0.58
Profile 3	Oe	0–6	–	–	–	–	–	–	–	–	–	–	–
	O/C	6–25	7484	3265	1865	1888	70	141	4219	1400	0.44	0.57	0.28
	AC	25–40	10352	5191	2789	2565	83	184	5160	2402	0.50	0.54	0.40
	BC	40–60	12100	5502	2650	2719	80	189	6598	2852	0.45	0.48	0.40
Profile 4	Oi	0–1	–	–	–	–	–	–	–	–	–	–	–
	A	1–13	19396	8545	2490	1371	147	344	10851	6055	0.44	0.29	0.26
	C1	13–35	31553	12213	1446	836	148	623	19340	10767	0.39	0.12	0.16
	C2	35–60	33188	13115	1780	848	146	723	20073	11334	0.40	0.14	0.17
Profile 5	Oe	0–3	–	–	–	–	–	–	–	–	–	–	–
	Oa	3–10	–	–	–	–	–	–	–	–	–	–	–
	A	10–15	35965	11425	4766	1152	63	449	24539	6659	0.32	0.42	0.35
	Bw	15–20	47532	10233	5522	1116	106	1267	37298	4711	0.22	0.54	0.39
	C	20–45	43194	7461	4460	542	156	1115	35733	3001	0.17	0.60	0.28
Profile 6	Oe	0–2	–	–	–	–	–	–	–	–	–	–	–
	Oa	2–10	–	–	–	–	–	–	–	–	–	–	–
	ABw	10–20	37929	8986	4928	1438	128	1542	28943	4058	0.24	0.55	0.39
	C	20–65	37223	7758	3974	340	130	990	29464	3785	0.21	0.51	0.23
Profile 7	Oe	0–2	–	–	–	–	–	–	–	–	–	–	–
	AC	2–15	30094	10122	7170	4478	138	226	19972	2952	0.34	0.71	0.81
	C	15–50	38044	9407	2962	4006	469	910	28637	6445	0.25	0.31	0.55
Profile 8	Oe	0–4	–	–	–	–	–	–	–	–	–	–	–
	AC	4–15	45015	19289	2035	613	37	2125	25726	17254	0.43	0.11	0.16
	C1	15–35	46457	17182	1781	625	54	4521	29275	15400	0.37	0.10	0.15
	C2	35–55	45016	19709	1298	723	45	3867	25307	18410	0.44	0.07	0.14
Profile 9	Oi	0–1	–	–	–	–	–	–	–	–	–	–	–
	AC	2–10	42267	17032	2056	1265	95	2986	25235	14976	0.40	0.12	0.23
	C1	10–40	45117	15404	2462	2639	321	3549	29714	12942	0.34	0.16	0.39
	C2	40–80	44167	16350	1950	2119	250	3487	27817	14400	0.37	0.12	0.31

Table 3 – continue

Profile	Horizon	Depth	Fe_t	Fe_d	Fe_{ox}	Al_{ox}	Si_{ox}	Mn_{ox}	$Fe_t - Fe_d$	$Fe_d - Fe_{ox}$	Fe_d/Fe_t	Fe_{ox}/Fe_d	$Al_{ox} + ½Fe_{ox}$
			mg·kg^{-1}										(%)
Profile 10	Oi	0–1	–	–	–	–	–	–	–	–	–	–	–
	AC	1–10	46208	16665	2273	1358	103	2209	29543	14392	0.36	0.14	0.25
	C1	10–50	43335	14692	3588	2190	161	2473	28642	11104	0.34	0.24	0.40
	C2	50–70	41660	14588	5273	3346	244	2458	27073	9314	0.35	0.36	0.60
Profile 11	Oi	0–1	–	–	–	–	–	–	–	–	–	–	–
	A	1–15	150180	44380	55275	3131	2933	3298	105801	–10895	0.30	1.25	3.08
	C1	15–30	166565	50639	71156	3474	3694	5656	115926	–20517	0.30	1.41	3.91
	C2	30–45	286041	48733	86147	4359	6149	5716	237308	–37414	0.17	1.77	4.74
	C3	45–60	311685	41840	90804	4369	5648	3500	269845	–48964	0.13	2.17	4.98
Profile 12	Oi	0–1	–	–	–	–	–	–	–	–	–	–	–
	A	1–20	189182	47390	74844	3680	2845	2876	141792	–27454	0.25	1.58	4.11
	C1	20–28	39962	12751	16693	1703	510	880	27211	–3942	0.32	1.31	1.00
	2C	28–50	344307	49050	93449	3810	4405	2142	295257	–44400	0.14	1.91	5.05
	3C	50–60	217413	49395	20469	500	1346	2649	168018	28926	0.23	0.41	1.07
	4C	60–75	27981	10311	8232	1407	324	500	17670	2079	0.37	0.80	0.55
Profile 13	Oi	0–1	–	–	–	–	–	–	–	–	–	–	–
	AC	1–15	16008	3690	3256	9615	11146	13961	12318	434	0.23	0.88	1.12
	2C	15–25	13457	1273	499	232	217	156	12184	774	0.09	0.39	0.05

Explanations: – not determined; Al_{ox} – oxalate-extractable Al; Fe_d – dithionite-extractable Fe; Fe_d/Fe_t – Fe oxide mobility index; Fe_{ox} – oxalate-extractable Fe; Fe_{ox}/Fe_d – Fe oxide activity index; Fe_t – total content of Fe; Mn_{ox} – oxalate-extractable Mn; Si_{ox} – oxalate-extractable Si.

4. Discussion

4.1. Micromorphological and submicromorphological indicators of pedogenesis

The Technosols studied were soils representing an initial stage of advancement of soil-forming processes, which is corroborated by a poor development of soil profiles. However, microscale effects of pedogenic transformation and reorganisation of soil substrate can be distinguished in these soils, which can be treated as micromorphological indicators of pedogenesis. These indicators show that despite the young age of soils (approximately 200–500 years) and poor soil profile development, the weathering, soil-forming, and biological processes transform technogenic mineral substrate into a functioning soil. The following micromorphological effects of pedogenesis were identified in the investigated Technosols: (1) sulphide weathering and formation of Fe oxide pseudomorphs after sulphides; (2) formation of pedogenic structure; (3) formation of pedogenic carbonate coatings in soils developed from mine wastes composed of carbonate rocks; (4) formation of pedogenic Fe and Mn oxide coatings in acidic soils developed from mine wastes composed of crystalline rocks (granite, gneiss); (5) formation of pedogenic sulphate coatings in soils containing metallurgical wastes, and (6) bioturbations and the formation of a soil material reworked by soil animals within biogenic channels.

The occurrence of Fe oxide pseudomorphs after sulphides (Fig. 2A and B; Fig. 6), particularly in profiles containing primary sulphides (i.e. in profiles 1–10), is clear evidence of active chemical weathering, which is the most important process involved in the transformation of Fe sulphides in the studied soils. This process was previously identified in Technosols (e.g. Néel et al., 2003; Uzarowicz and Skiba, 2011; Uzarowicz et al., 2024), and is expressed by the development of pseudomorphs due to the gradual in situ transformation of sulphides into Fe oxides through the oxidation of sulphides, accompanied by the release of sulphate ions to the soil solution. It was found in previous studies of Technosol chronosequence that the degree of sulphide transformation and the crystallinity of iron oxides increase with soil age (Uzarowicz, 2013). Both Fe sulphides and Fe oxide pseudomorphs after sulphides were rare components of the studied Technosols in the Tatra Mountains. The majority of pseudomorphs found in these soils were totally composed of Fe oxides, which suggests that Technosols containing primary sulphides (i.e., in profiles 1–10) were well aerated soils. It is due to a considerable content of rock fragments in these soils (Table 1),

which enables the air exchange in the studied soils and the oxidation of sulphides (Hayes et al., 2014).

Micromorphological analysis showed the initial development of soil structure, particularly the aggregation of primary particles into soil aggregates (Figs 1–4). The presence of intergrain microaggregate microstructure between rock fragments in the soil indicates the beginning of pedogenic aggregation in the studied Technosols in the Tatra Mountains. Previous studies show that Technosols originate from technogenic substrates such as coal/lignite combustion ashes or mine wastes, which initially have a firm consistency with little aggregation (Uzarowicz et al. 2018a, 2025; Watteau et al., 2019). Soil structure formation begins in the first few years of soil development (Badin et al., 2009; Séré et al., 2010), primarily in the topsoil, as vegetation emerges on a disposal site and the organic matter accumulates in superficial soil horizons. The accumulation of soil organic matter (SOM) is crucial for the development of stable soil aggregates that improve soil structure (Jangorzo et al., 2013, 2014; Watteau et al., 2019). Ortega et al. (2022) found that between 15 and 40 years, the Technosols exhibit advanced structural development and nutrient content comparable to those of natural soils. Biological processes including plant root growth and fauna activity, promote the formation of soil aggregates and increase soil porosity (Hedde et al., 2019). Moreover, the abundance of Ca and carbonates in Technosols also plays a huge role in the development of soil structure (Uzarowicz et al., 2018b). Calcium is most likely an important structure-forming factor in carbonate-rich Technosols in the Tatra Mountains.

Another indicator of pedogenesis in the investigated Technosols is the formation of pedogenic carbonates. Secondary carbonate coatings were identified both micromorphologically (Fig. 1G and H) and by SEM-EDS in Technosols rich in carbonates occurring originally in mine wastes (Fig. 6). Pedogenic carbonates result from the precipitation of $CaCO_3$ from percolating soil solutions, often following the dissolution of primary carbonates (Zamanian et al., 2016; Kowalska et al., 2020). Pedogenic Ca carbonates were previously found, for example, in Technosols developed from thermal power station ash (Uzarowicz et al., 2017; Uzarowicz et al., 2018a; Konstantinov et al., 2020) and in Technosols developing from iron industry deposits (Huot et al., 2014b). Moreover, pedogenic Cu carbonates were identified in Technosols developed from mine wastes from historical copper mines (Uzarowicz et al., 2024). The occurrence of pedogenic carbonates in technogenic soils is evidence of the weathering of Ca-rich technogenic materials and the crystallisation of secondary carbonates from soil solution.

Distinct Fe oxide coatings on mineral grains and rock fragments were observed in acidic Technosols (Fig. 3A and B). The coatings were frequently found in profiles 5 and 6 in A, Bw, and ABw horizons. Such coatings indicate podzolisation and chemical weathering (Van Ranst et al., 2018) involving mobilisation and subsequent precipitation of Fe oxides and oxyhydroxides. Pedogenic Fe oxide coatings in acidic soils arise through the release of Fe from primary Fe-bearing minerals, Fe oxidation, and the precipitation of Fe oxides and oxyhydroxides (Cornell and Schwertmann, 2003). This process is influenced by biological activity, redox conditions, and soil chemical properties. As a result, Fe oxides accumulate as coatings on soil particles. Fe oxide coatings occurring in Technosols containing Bw horizons indicate that pedogenesis in these soils is so advanced that there are conditions for Fe mobilization and Fe oxide coating formation. Technosols with Bw horizons are located in the Pyszniańska Valley, where mining was carried out most likely in the 15th century (Table 1). Therefore, the formation of Bw horizons containing Fe oxide coatings may be related to a relatively long pedogenesis period (Tarnawczyk et al., 2024).

The Mn oxide coatings, which seem to be pedogenic in origin, although less common, were also identified in acidic Technosols (Fig. 7). The explanation of the formation of Mn oxide coatings in the studied Technosols is difficult. Although Mn oxide/hydroxide minerals (e.g., birnessite) are ubiquitous in soils and sediments (McKenzie, 1989), studies on the formation/synthesis of the manganese minerals as coatings in soils are limited (e.g., Eswaran and Raghu Mohan, 1973; Sullivan and Koppi, 1992; Eren et al., 2014). The interplay of soil pH, redox conditions, and biological activity controls Mn oxide precipitation dynamics in soils (Mayanna et al., 2015). Higher pH generally enhances abiotic Mn oxide precipitation, as it was found in Technosols developing from iron industry deposits (Huot et al., 2014b), whereas at lower soil pH, microbial oxidation often drives Mn oxide formation (Mayanna et al., 2015). Therefore, we hypothesize that the formation of Mn oxide coatings in acidic Technosols in the Tatra Mountains can be related to microbial activity in the soils.

In Technosols containing metallurgical wastes, coatings composed of sulphates were identified on mineral grains (Fig. 8), likely resulting from the release of sulphur during the weathering of metallurgical wastes. This is consistent with a number of studies focused on the effects of weathering of metallurgical slags in environmental conditions (Kierczak et al., 2021). Technosols containing metallurgical wastes were rich in anthropogenic organic matter occurring as charcoals. They are the remnants of past industrial activities related to smelting. Similar findings were presented by Huot et al. (2014a). Although slags are anthropogenic materials (Warchulski et al., 2020), they undergo natural weathering processes similar to weathering of minerals and rocks (Kierczak et al., 2021). Weathering transforms primary crystalline phases and glassy (amorphous) components, altering their mineral and chemical composition over time. Secondary minerals such as carbonates, hydroxides, or sulfate-bearing phases may precipitate as coatings or fill voids in slag particles. Sulphate formation during slag weathering arises from the oxidation of sulphide minerals originally occurring in slags, leading to the generation of sulphate ions that precipitate as secondary sulphate minerals (e.g., gypsum). These sulphates are common weathering products indicative of advanced alteration of metallurgical slags (Kierczak et al., 2021). Moreover, weathering of metallurgical slags leads to the mobilisation of metals such as Zn, Pb, Cu, and As, which can be hazardous to the local environment (Kierczak et al., 2013; Potysz et al., 2018; Tarnawczyk et al., 2025).

Evidence of biological activity, including faunal channels, presence of soil fauna (nematodes or enchytraeids) and roots, was identified in several Technosols under study (Fig. 1A, 3G,

4A, and 5C), in particular those with higher organic matter content or plant residues, which is consistent with previous studies (Arocena et al., 2010). As it was mentioned above, biological factors such as root penetration and bioturbation contribute to the formation of soil structure. Biological colonisation of post-industrial areas including industrial waste disposal sites, accelerates aggregate formation and soil structure differentiation (Santini and Fey, 2016; Domínguez-Haydar et al. 2018; Uzarowicz et al., 2020b). The presence of soil fauna (nematodes or enchytraeids) found in voids in slag particles in Technosols containing metallurgical wastes (Fig. 4A and B) indicates that the slags, which are strongly contaminated with trace elements (e.g. Cu, As and Sb) (Tarnawczyk et al., 2025) and seem to be an unfavourable place for living organisms, can be colonised by fauna and serve as a habitat for soil animals. This is in contrast to previous studies (e.g. Acosta et al., 2011) in which the authors found that the soil fauna is vulnerable to high concentrations of trace elements.

4.2. Selective extractions of Fe, Al, Si, and Mn as chemical indicators of pedogenesis

Analysis of Fe, Al, Si, and Mn forms in the studied Technosols from the Tatra Mountains revealed a great diversity of the forms, depending most likely on the nature of anthropogenic parent material. A similar feature was identified in other Technosols developed from diverse industrial wastes (Uzarowicz and Skiba, 2011; Uzarowicz et al., 2017, 2024, 2025).

Pedogenic forms of Fe and Al in the Spolic Technosols studied indicate that in acidic soils, especially those developed from silicate-derived mining wastes, pedogenic processes lead to the mobilisation of Fe and Al. In acidic soils, increased concentrations of oxalate-extracted forms of Fe and Al were identified, which is characteristic of the initial stages of podzolisation and chemical weathering (McKeague and Day, 1966; Krettek and Rennert, 2021). Such a phenomenon has been documented in studies conducted on technogenic acidic soils, where weathering of primary minerals (e.g., biotite, muscovite, plagioclase) leads to the release of Fe and Al into the soil solution, and subsequent precipitation as amorphous or poorly crystalline oxides and hydroxides (Kalita et al., 2019). Similar results were obtained in studies of Technosols in Poland on historical copper mine dumps in Miedziana Góra and Miedzianka (Uzarowicz et al., 2024) as well as on iron ore mine dumps at Osicowa Góra (Uzarowicz et al., 2025) confirming the beginning of Fe and Al mobilisation at the early stages of pedogenesis.

Very high concentrations of oxalate-extractable Mn were detected in profiles 1 and 2, which is most likely related to a high content of Mn in the parent material. Elevated Mn_{ox} content in the investigated soils may indicate active redox cycles and microbial involvement in the oxidation of Mn (Mayanna et al., 2015). In turn, the mobilisation of silicon (Si_{ox}) is associated with the weathering of primary silicate minerals and the formation of secondary amorphous Si forms, which seem to be typical for the early stages of technogenic soils (Uzarowicz et al., 2024, 2025). Concentrations of oxalate-extractable Al and Si were higher in Technosols containing metallurgical slags than in other soils studied (Table 3). This feature is most likely related to the weathering of slags accompanied by a release of Al and Si from slags. Oxalate-extractable Al and Si release was documented during pedogenesis in Technosols developed from thermal power station ash and slag (Uzarowicz et al., 2017), which reflects mineral transformations of ash and slag in the soil environment.

Very high concentrations of oxalate-extractable Fe (Fe_{ox}) are recorded in Technosols containing metallurgical wastes, especially those containing magnetite-rich slags (profiles 11 and 12). Concentrations of Fe_{ox} in these soils are higher than Fe_d (Table 3), which is an unusual situation in the soil environment. A similar phenomenon was identified in Technosols developed from thermal power station ash (Uzarowicz et al., 2017), where it was shown that high Fe_{ox} content does not always reflect only the presence of pedogenic, amorphous forms of Fe, but may also originate from amorphous Fe present in the parent material or be an artefact of the extraction method in the presence of magnetite. This is a mineral that is partially dissolved during dithionite and oxalate extractions (Walker, 1983; Fine and Singer, 1989; Van Oorschot and Dekkers, 1999). Therefore, once magnetite is present in soil, it is difficult to draw reliable conclusions from selective extractions of Fe.

5. Conclusions

1. Micromorphological observations and selective Fe, Al, Si and Mn extractions confirm the initial effects of pedogenesis in Spolic Technosols in areas of historical mining and smelting in the Tatra Mountains. This shows that soils in human-altered high-mountain environments undergo soil-forming processes and may acquire functional properties and ecological significance within a few centuries of pedogenesis.
2. The occurrence of occasional Fe oxide pseudomorphs after sulphides shows that there are good conditions for sulphide weathering in the studied Technosols due to good soil aeration.
3. Soil structure development in the studied Technosols is influenced by weathering of rocks and mineral transformations, chemical properties (e.g. presence or lack of carbonates), organic matter accumulation in the topsoil, as well as root penetration and bioturbation of fauna.
4. Pedogenic coatings reflect the geochemical properties of the parent materials. In soils developed from carbonate-bearing mine wastes, pedogenic carbonate coatings formed due to partial dissolution of primary carbonates and subsequent recrystallisation. In acidic soils derived from crystalline rocks (granite, gneiss), iron oxide coatings were common in Bw horizons, indicating Fe mobilisation and precipitation as Fe oxyhydroxides, whereas Mn oxide coatings occurred only sporadically and formed most likely due to microbial activity. In soils containing metallurgical slags, sulphate coatings were observed, most likely resulting from slag weathering, sulphur release into the soil solution, and crystallisation of sulphates on mineral grains.

5. Bioturbations were observed in the majority of the studied Technosols. These pedofeatures were represented by root channels and biogenic channels filled with a material reworked by soil animals. Soil animals (most likely nematodes or enchytraeids) were found in voids of metallurgical slag, which indicates favourable conditions for the development of fauna communities in Technosols containing wastes from smelting activities.
6. Selective extraction methods showed the release of oxalate-extractable Mn in soils developed from Mn-bearing ore mine wastes, a slight mobilisation of oxalate-extractable Fe and Al in acidic Technosols developed from aluminosilicate parent material (granite, gneiss), and the release of oxalate-extractable Al and Si in Technosols containing metallurgical slags.

CRediT authorship contribution statement

Magdalena Tarnawczyk: Writing original draft, Writing– review & editing, Visualization, Validation, Project administration, Methodology, Investigation, Funding acquisition, Data curation, Conceptualization. **Łukasz Uzarowicz:** Writing– original draft, Writing– review & editing, Validation, Supervision, Methodology, Investigation, Funding acquisition, Data curation, Conceptualization. **Artur Pędziwiatr:** Writing– review & editing, Validation, Methodology, Investigation, Conceptualization. **Wojciech Kwasowski:** Writing– review & editing, Validation, Supervision, Methodology, Investigation, Conceptualization.

Declaration of competing interest

The authors declare that they have no known competing financial interests or personal relationships that could have appeared to influence the work reported in this paper.

Acknowledgments

This work was supported by the National Science Centre, Poland, under research project no. 2021/41/N/ST10/03129. The Minister of Climate and Environment, as well as the Director of the Tatra National Park (TNP), are acknowledged for the permission to conduct the studies in the TNP. Maria Król and Magdalena Sitarz (TNP), as well as Arletta Kochańska-Jeziorska, are acknowledged for their help in the fieldwork and in finding the literature related to the topic. Jakub Kotowski and Marcin Łącki (Faculty of Geology, University of Warsaw, Poland) are acknowledged for their assistance with SEM-EDS analyses.

References

Acosta, J.A., Martinez-Martinez, S., Faz, A., Mourik, J.M. Van, Arocena, J.M., 2011. Micromorphological and chemical approaches to understand changes in ecological functions of metal-impacted soils under various land uses. Applied and Environmental Soil Science 2011, 521329. https://doi.org/10.1155/2011/521329

Allory, V., Séré, G., Ouvrard, S., 2022. A meta-analysis of carbon content and stocks in Technosols and identification of the main governing factors. European Journal of Soil Science 73(1), e13141. https://doi.org/10.1111/ejss.13141

Arocena, J., Mourik, J.M., Schilder, M., Faz Cano, A., 2010. Initial soil development under pioneer plant species in metal mine waste deposits. Restoration Ecology 18, 244–252. https://doi.org/10.1111/j.1526-100X.2009.00582.x

Badin, A.L., Méderel, G., Béchet, B., Borschneck, D., Delolme, C., 2009. Study of the aggregation of the surface layer of Technosols from stormwater infiltration basins using grain size analyses with laser diffractometry. Geoderma 153, 163–171. https://doi.org/10.1016/j.geoderma.2009.07.022

Castillo Corzo, M., Peña Rodríguez, V., Manrique Nugent, M., Villarreyes Peña, E., Byrne, P., Gonzalez, J.C., Patiño Camargo, G., Barnes, C.H.W., Sánchez Ortiz, J.F., Saldaña Tovar, J., De Los Santos Valladares, L., 2025. Potentially toxic elements and radionuclides contamination in soils from the vicinity of an ancient mercury mine in Huancavelica, Peru. Soil Science Annual 76(2), 204389. https://doi.org/10.37501/soilsa/204389

Charzyński, P., Hulisz, P., Bednarek, R.M. (Eds.), 2013. Technogenic soils of Poland. Torun, Polish Society of Soil Science.

Colombini, G., Auclerc, A., Watteau, F., 2020. Techno-moder: A proposal for a new morpho-functional humus form developing on Technosols revealed by micromorphology. Geoderma 375, 114526. https://doi.org/10.1016/j.geoderma.2020.114526

Cornell, R.M., Schwertmann, U., 2003. The Iron Oxides: Structure, Properties, Reactions, Occurrences and Uses, Second Edition. Wiley-VCH Verlag.

Díaz-Ortega, J., Rivera-Uria, Y., López-Mendoza, E., Sedov, S., Romero, F., Solleiro-Rebolledo, E., Martínez-Jardines, L.G., 2024. Development of sustainable hydromorphic Technosols within artificial wetlands in mining landscapes: the effects of wastewater and hydrothermal geological materials. Journal of Soils and Sediments 24, 2948–2962. https://doi.org/10.1007/s11368-024-03763-4

Domínguez-Haydar, Y., Castañeda, C., Rodríguez-Ochoa, R., Jiménez, J.J., 2018. Assessment of soil fauna footprints at a rehabilitated coal mine using micromorphology and near infrared spectroscopy (NIRS). Geoderma 313, 135–145. https://doi.org/10.1016/j.geoderma.2017.10.032

Drewnik, M., 2008. Geomorfologiczne uwarunkowania rozwoju pokrywy glebowej w obszarach górskich na przykładzie Tatr. Wydawnictwo UJ. (in Polish)

Drewnik, M., Felisiak, I., Jerzykowska, I., Magiera, J., 2008. The Tatra Mts: rocks, landforms, weathering and soils. Geotourism/Geoturystyka 2(13), 51–74. https://doi.org/10.7494/geotour.2008.13.51

Eren, M., Kadir, S., Zucca, C., Akşit, İ., Kaya, Z., Kapur, S., 2014. Pedogenic manganese oxide coatings (calcium buserite) on fracture surfaces in Tortonian (Upper Miocene) red mudstones, southern Turkey. Catena 116, 149–156. https://doi.org/10.1016/j.catena.2014.01.003

Eswaran, H., Raghu Mohan, G., 1973. The microfabric of petroplinthite. Soil Science Society of America Proceedings 37, 79–82. https://doi.org/10.2136/sssaj1973.03615995003700010027x

Fine, P., Singer, M.J., 1989. Contribution of ferrimagnetic minerals to oxalate- and dithionite-extractable iron. Soil Science Society of America Journal 53, 191–196.

Gradziński, M., Jach, R., Stworzewicz, E., 2001. Origin of calcite-cemented Holocene slope breccias from the Długa Valley (the Western Tatra Mountains). Annales Societatis Geologorum Poloniae 71(2), 105–113.

Grünewald, G., Kaiser, K., Jahn, R., 2007. Alteration of secondary minerals along a time series in young alkaline soils derived from carbonatic wastes of soda production. Catena 71(3), 487–496. https://doi.org/10.1016/j.catena.2007.03.022

Hayes, S.M., Root, R.A., Perdrial, N., Maier, R.M., Chorover, J., 2014. Surficial weathering of iron sulfide mine tailings under semi-arid climate. Geochimica et Cosmochimica Acta 141, 240–257. https://doi.org/10.1016/j.gca.2014.05.030

Hedde, M., Nahmani, J., Séré, G., Auclerc, A., Cortet, J., 2019. Early colonization of constructed Technosols by macro-invertebrates. Journal of Soils and Sediments 19, 3193–3203. https://doi.org/10.1007/s11368-018-2142-9

Hess, M., 1996. Climate. [In:] Mirek, Z., Głowaciński, Z., Klimek, K., Piękoś-Mirkowa, H. (Eds.), Nature of the Tatra National Park. Tatrzański Park Narodowy, Kraków-Zakopane, pp. 53–68.

Huot, H., Faure, P., Biache, C., Lorgeoux, C., Simonnot, M.O., Morel, J.L., 2014a. A Technosol as archives of organic matter related to past industrial activities. Science of the total Environment, 487, 389–398. https://doi.org/10.1016/j.scitotenv.2014.04.047

Huot, H., Simonnot, M.O., Watteau, F., Marion, P., Yvon, J., De Donato, P., Morel, J.L., 2014b. Early transformation and transfer processes in a Technosol developing on iron industry deposits. European Journal of Soil Science 65, 470–484. https://doi.org/10.1111/ejss.12106

Huot, H., Simonnot, M.O., Morel, J.L., 2015. Pedogenetic trends in soils formed in technogenic parent materials. Soil Science 180(4/5), 182–192. https://doi.org/10.1097/SS.0000000000000135

IUSS Working Group WRB, 2022. World Reference Base for Soil Resources. International soil classification system for naming soils and creating legends for soil maps. 4th edition. International Union of Soil Sciences (IUSS), Vienna, Austria.

Jangorzo, N.S., Watteau, F., Schwartz, C., 2013. Evolution of the pore structure of constructed Technosol during early pedogenesis quantified by image analysis. Geoderma 207−208, 180−192. https://doi.org/10.1016/j.geoderma.2013.05.016

Jangorzo, N.S., Schwartz, C., Watteau, F., 2014. Image analysis of soil thin sections for a non-destructive quantification of aggregation in the early stages of pedogenesis. European Journal of Soil Science 65(4), 485−498. https://doi.org/10.1111/ejss.12110

Jost, H., 1962. O górnictwie i hutnictwie w Tatrach Polskich. Wyd. Nauk.-Techn. Warszawa, pp. 186. (in Polish)

Jost, H., 2004. Dzieje górnictwa i hutnictwa w Tatrach Polskich. Zakopane. (in Polish)

Kabała, C., Greinert, A., Charzyński, P., Uzarowicz, Ł., 2020. Technogenic soils – soils of the year 2020 in Poland. Concept, properties and classification of technogenic soils in Poland. Soil Science Annual 71(4), 267–280. https://doi.org/10.37501/soilsa/131609

Kalita, P., Dutta, M., Karmakar, R.M., Dutta, S., Deka, B., 2019. Pedogenic distribution of iron and aluminium under different land uses in Golaghat district of Assam. Journal of Pharmacognosy and Phytochemistry 8(3), 2554–2561.

Krettek, A., Rennert, T., 2021. Mobilisation of Al, Fe, and DOM from topsoil during simulated early Podzol development and subsequent DOM adsorption on model minerals. Scientific Reports 11, 19741. https://doi.org/10.1038/s41598-021-99365-y

Kierczak, J., Pietranik, A., Piatak, N.M., 2021. Weathering of Slags. [In:] Piatak N.M., Ettler, V. (Eds.), Metallurgical Slags: Environmental Geochemistry and Resource Potential, The Royal Society of Chemistry, pp. 125–150.

Kierczak, J., Potysz, A., Pietranik, A., Tyszka, R., Modelska, M., Néel, C., Ettler, V., Mihaljevič, M., 2013. Environmental impact of the historical Cu smelting in the Rudawy Janowickie Mountains (south-western Poland). Journal of Geochemical Exploration 124, 183–194. https://doi.org/10.1016/j.gexplo.2012.09.008

Klimaszewski, M., 1996. Geomorphology. [In:] Mirek, Z., Głowaciński, Z., Klimek, K., Piękoś-Mirkowa, H. (Eds.), Nature of the Tatra National Park. Tatrzański Park Narodowy, Kraków-Zakopane, pp. 97–124.

Konstantinov, A., Novoselov, A., Konstantinova, E., Loiko, S., Kurasova, A., Minkina, T., 2020. Composition and properties of soils developed within the ash disposal areas originated from peat combustion (Tyumen, Russia). Soil Science Annual 71(1), 3–14. https://doi.org/10.37501/soilsa/121487

Komornicki, T., Skiba, S., 1996. Gleby, in: Mirek, Z., Głowaciński, Z., Klimek, K., Piękoś-Mirkowa, H. (Eds.), Przyroda Tatrzańskiego Parku Narodowego. Tatrzański Park Narodowy, Kraków-Zakopane, pp. 215–229.

Kotański, Z., 1971. Przewodnik geologiczny po Tatrach. Wydawnictwo Geologiczne, Warszawa. (in Polish)

Kowalska, J.B., Zaleski, T., Mazurek, R., 2020. Micromorphological features of soils formed on calcium carbonate-rich slope deposits in the Polish Carpathians. Journal of Mountain Science 17(6), 1310–1332. https://doi.org/10.1007/s11629-019-5829-5

Liberak, M., 1927. Górnictwo i hutnictwo w Tatrach Polskich. Wierchy 5, 13–30. (in Polish)

Mayanna, S., Peacock, C.L., Schäffner, F., Grawundera, A., Mertena, D., Kothec, E., Büchela, G., 2015. Biogenic precipitation of manganese oxides and enrichment of heavy metals at acidic soil pH. Chemical Geology 402, 6–17. https://doi.org/10.1016/j.chemgeo.2015.02.029

McKeague, J.A., Day, J.H., 1966. Dithionite- and oxalate-extractable Fe and Al as aids in differentiating various classes of soils. Canadian Journal of Soil Science 46(1), 13–22. https://doi.org/10.4141/cjss66-003

McKenzie, R.M., 1989. Manganese oxides and hydroxides. [In:] Dixon, J.B., Weed, S.B. (Eds.), Minerals in Soil Environments, Soil Science Society of America. Madison, WI, pp. 439–461.

Mehra, O.P., Jackson, M.L., 1958. Iron oxide removal from soils and clay by a dithionite-citrate system buffered with sodium bicarbonate. Clays and Clay Minerals 7, 317–327. https://doi.org/10.1346/CCMN.1958.0070122

Miechówka, A., Ciarkowska, K., 1998. Mikromorfologiczne formy próchnicy tatrzańskich rędzin próchnicznych i butwinowych. Zeszyty Problemowe Postępów Nauk Rolniczych 464, 161–168. (in Polish)

Mirek, Z., 1996. Antropogenic threats and changes of the nature. [In:] Mirek, Z., Głowaciński, Z., Klimek, K., Piękoś-Mirkowa, H. (Eds.), Nature of the Tatra National Park. Tatrzański Park Narodowy, Kraków-Zakopane, pp. 595–618.

Néel, C., Bril, H., Courtin-Nomade, A., Dutreuil, J.P., 2003. Factors affecting natural development of soil on 35-year-old sulphide-rich mine tailings. Geoderma 111, 1–20. https://doi.org/10.1016/S0016-7061(02)00237-9

Ortega, J., Sedov, S., Romero, F., Jardines, L., Solleiro-Rebolledo, E., 2022. Chronosequence of Technosols at the Peña Colorada mine in Colima, Mexico: a short-term remediation alternative. Journal of Soils and Sediments 22, 942–956. https://doi.org/10.1007/s11368-021-02990-3

Osika, R., 1987. Budowa geologiczna Polski, t. IV Złoża surowców mineralnych. Wydawnictwo Geologiczne, Warszawa. (in Polish)

Pansu, M., Gautheyrou, J., 2006. Handbook of Soil Analysis. Mineralogical, Organic and Inorganic Methods. Springer Berlin, Heidelberg.

Passendorfer, E., 1996. Geology. [In:] Mirek, Z., Głowaciński, Z., Klimek, K., Piękoś-Mirkowa, H. (Eds.), Nature of the Tatra National Park. Tatrzański Park Narodowy, Kraków-Zakopane, pp. 69–96.

Piękoś-Mirkowa, H., Mirek, Z., 1996. Zbiorowiska roślinne, in: Mirek, Z., Głowaciński, Z., Klimek, K., Piękoś-Mirkowa, H. (Eds.), Przyroda Tatrzańskiego Parku Narodowego. Tatrzański Park Narodowy, Kraków-Zakopane, pp. 237–274.

Potysz, A., Kierczak, J., Grybos, M., Pędziwiatr, A., van Hullebusch, E.D., 2018. Weathering of historical copper slags in dynamic experimental system with rhizosphere-like organic acids. Journal of Environmental Management 222, 325–337. https://doi.org/10.1016/j.jenvman.2018.05.071

Radwańska-Paryska, Z., Paryski, W.H., 1995. Wielka Encyklopedia Tatrzańska. Wyd. Górskie, Poronin, pp. 1555.

Rączkowska, Z.J., 2019. Human impact in the Tatra Mountains. Cuadernos de investigación geográfica / Geographical Research Letters 45(1), 219–244.

Ruiz, F., Andrade, G.R.P., Sartor, L.R., Santos, J.C.B. dos, Souza Júnior, V.S. de, Ferreira, T.O., 2022. The rhizosphere of tropical grasses as driver of soil weathering in embryonic Technosols (SE-Brazil). Catena 208, 105764. https://doi.org/10.1016/j.catena.2021.105764

Santini, T.C., Fey, M.V., 2016. Assessment of Technosol formation and in situ remediation in capped alkaline tailings. Catena 136, 17–29. https://doi.org/10.1016/j.catena.2015.08.006

Schwertmann, U., 1964. Differenzierung der Eisenoxide des Bodens durch photochemische Extraktion mit saurer Ammoniumoxalat-Lösung. Zeitschrift für Pflanzenernährung und Bodenkunde 105, 194–202.

Séré, G., Schwartz, C., Ouvrard, S., Renat, J.C., Watteau, F., Villemin, G., Morel, J.L., 2010. Early pedogenic evolution of constructed Technosols. Journal of Soils and Sediments 10, 1246–1254. https://doi.org/10.1007/s11368-010-0206-6

Soil Science Division Staff, 2017. Soil Survey Manual. Ditzler, C., Scheffe, K., Monger H.C. (Eds.) USDA Handbook 18. Washington, D.C.

Stoops, G., 2021. Guidelines for analysis and description of soil and regolith thin sections. John Wiley & Sons, 184 p.

Stoops, G., Marcelino, V., Mees, F., 2018. Micromorphological features and their relation to processes and classification: general guidelines and Overview. [In:] Stoops, G., Marcelino, V., Mees, F. (Eds.), Interpretation of Micromorphological Features of Soils and Regoliths. Elsevier, pp. 15–35.

Sullivan, L.A., Koppi, A.J., 1992. Manganese oxide accumulations associated with some soil structural pores. I. Morphology, composition and genesis. Australian Journal of Soil Research 30(4), 409–427. https://doi.org/10.1071/SR9920409

Swęd, M., Uzarowicz, Ł., Duczmal-Czernikiewicz, A., Kwasowski, W., Pędziwiatr, A., Siepak, M., Niedzielski, P., 2022. Forms of metal (loid) s in soils derived from historical calamine mining waste and tailings of the Olkusz Zn–Pb ore district, southern Poland: A combined pedological, geochemical and mineralogical approach. Applied Geochemistry 139, 105218. https://doi.org/10.1016/j.apgeochem.2022.105218

Tarnawczyk, M., Uzarowicz, Ł., Kwasowski, W., Górka-Kostrubiec, B., Pędziwiatr, A., 2024. Soil-forming factors controlling Technosol formation in historical mining and metallurgical sites in the high-alpine environment of the Tatra Mountains, southern Poland. Catena 247, 108521. https://doi.org/10.1016/j.catena.2024.108521

Tarnawczyk, M., Uzarowicz, Ł., Kwasowski, W., Pędziwiatr, A., Martín-Peinado, F.J., 2025. Geochemical features of Technosols developed in historical mining and metallurgical sites in the Tatra Mountains, southern Poland: total contents and BCR fractionation of selected trace elements. Minerals 15, 988. https://doi.org/10.3390/min15090988

Thompson, R., Oldfield, F., 1986. Environmental Magnetism. Allen and Unwin, London. https://doi.org/10.1007/978-94-011-8036-8

Uzarowicz, Ł., 2013. Microscopic and microchemical study of iron sulphide weathering in a chronosequence of technogenic and natural soils. Geoderma 197, 137–150. https://doi.org/10.1016/j.geoderma.2013.01.006

Uzarowicz, Ł., Skiba, S., 2011. Technogenic soils developed on mine spoils containing iron sulphides: Mineral transformations as an indicator of pedogenesis. Geoderma 163(1–2), 95–108. https://doi.org/10.1016/j.geoderma.2011.04.008

Uzarowicz, Ł., Zagórski, Z., Mendak, E., Bartmiński, P., Szara, E., Kondras, M., Oktaba, L., Turek, A., Rogoziński, R., 2017. Technogenic soils (Technosols) developed from fly ash and bottom ash from thermal power stations combusting bituminous coal and lignite. Part I. Properties, classification, and indicators of early pedogenesis. Catena 157C, 75–89. https://doi.org/10.1016/j.catena.2017.05.010

Uzarowicz, Ł., Kwasowski, W., Śpiewak, O., Świtoniak, M., 2018a. Indicators of pedogenesis of Technosols developed in an ash settling pond at the Bełchatów thermal power station (central Poland). Soil Science Annual 69(1), 49–59. https://doi.org/10.2478/ssa-2018-0006

Uzarowicz, Ł., Skiba, M., Leue, M., Zagórski, Z., Gąsiński, A., Trzciński, J., 2018b. Technogenic soils (Technosols) developed from fly ash and bottom ash from thermal power stations combusting bituminous coal and lignite. Part II. Mineral transformations and soil evolution. Catena 162, 255–269. https://doi.org/10.1016/j.catena.2017.11.005

Uzarowicz, Ł., Charzyński, P., Greinert, A., Hulisz, P., Kabała, C., Kusza, G., Kwasowski, W., Pędziwiatr, A., 2020a. Studies of technogenic soils in Poland: past, present, and future perspectives. Soil Science Annual 71(4), 281–299. https://doi.org/10.37501/soilsa/131615

Uzarowicz, Ł., Wolińska, A., Błońska, E., Szafranek-Nakonieczna, A., Kuźniar, A., Słodczyk, Z., Kwasowski, W., 2020b. Technogenic soils (Technosols) developed from mine spoils containing Fe sulphides: Microbiological activity as an indicator of soil development following land reclamation. Applied Soil Ecology 156, 103699. https://doi.org/10.1016/j.apsoil.2020.103699

Uzarowicz, Ł., Swęd, M., Kwasowski, W., Pędziwiatr, A., Kaczmarek, D., Koprowska, D., Górka-Kostrubiec, B., Pawłowicz, E., Murach, D., 2024. Initial pedogenic processes, mineral and chemical transformations and mobility of trace elements in Technosols on dumps of the former copper mines in Miedziana Góra and Miedzianka, the Świętokrzyskie Mts., south-central Poland. Catena 245, 108293. https://doi.org/10.1016/j.catena.2024.108293

Uzarowicz, Ł., Kwasowski, W., Lasota, J., Błońska, E., Górka-Kostrubiec, B., Tarnawczyk, M., Murach, D., Gilewska, M., Gryczan, W., Pawłowicz, E., Jankowski, P., 2025. Vegetation cover as an important factor affecting the properties and evolution of Spolic Technosols: A case study from a dump of the abandoned iron ore mine in central Poland. Catena 254, 108906. https://doi.org/10.1016/j.catena.2025.108906

Van Oorschot, I.H.M., Dekkers, M.J., 1999. Dissolution behaviour of fine-grained magnetite and maghemite in the citrate-bicarbonate-dithionite extraction method. Earth and Planetary Science Letters 167(3–4), 283–295.

Van Ranst, E., Wilson, M.A., Righi, D., 2018. Spodic Materials. [In:] Stoops, G., Marcelino, V., Mees, F. (Eds.), Interpretation of Micromorphological Features of Soils and Regoliths (Second Edition). Elsevier, pp. 633–662. https://doi.org/10.1016/B978-0-444-63522-8.00022-X

Van Reeuwijk, L.P., 2002. Procedures for soil analysis. Technical Paper 9. ISRIC, Wageningen.

Verrecchia, E.P., Trombino, L., 2021. A Visual Atlas for Soil Micromorphologists. Springer, Cham.

Walker, A., 1983. The effects of magnetite on oxalate- and dithionite-extractable iron. Soil Science Society of America Journal 47, 1022–1026.

Warchulski, R., Szczuka, M., Kupczak, K., 2020. Reconstruction of 16th–17th century lead smelting processes on the basis of slag properties: a case study from Sławków, Poland. Minerals 10(11), 1039. https://doi.org/10.3390/min10111039

Warzyński, H., Sosnowska, A., Harasimiuk, A., 2018. Effect of variable content of organic matter and carbonates on results of determination of granulometric composition by means of Casagrande's areometric method in modification by Prószyński. Soil Science Annual 69(1), 39–48. https://doi.org/10.2478/ssa-2018-0005

Watteau, F., Séré, G., Huot, H., Begin, J.C., Schwartz, C., Qiu, R., Morel, J.L., 2017. Micropedology of SUITMAs. [In:] Levin, M.J., Kim, K.-H.J., Morel, J.L., Burghardt, W., Charzyński, P., Shaw, R.K., IUSS Working Group SUITMA (Eds.), Soils within Cities, Global approaches to their sustainable management: Stuttgart, Germany, Catena Soil Sciences, Schweizerbart Science Publishers, pp. 84−92.

Watteau, F., Huot, H., Morel, J.-L., Rees, F., Schwartz, C., Séré, G., 2018. Micropedology to reveal pedogenetic processes in Technosols. Spanish Journal of Soil Science 8(2), 148–163. https://doi.org/10.3232/SJSS.2018.V8.N2.02

Watteau, F., Jangorzo, N.S., Schwartz, C., 2019. A micromorphological analysis for quantifying structure descriptors in a young constructed Technosol. Boletín de la Sociedad Geológica Mexicana 71(1), 11–20. https://doi.org/10.18268/bsgm2019v71n1a2

Watteau, F., Morel, J.L., Liu, C., Tang, Y., Huot, H., 2025. Technosol micromorphology reveals the early pedogenesis of abandoned rare earth element mining sites undergoing reclamation in south China. Minerals 15(5), 514. https://doi.org/10.3390/min15050514

Wątocki, W., 1950. Żyły mineralne na Ornaku w Tatrach Zachodnich. Annales Societatis Geologorum Poloniae 20(1–2), 11–60. (in Polish)

Woś, B., Tahsin Karimi Nezhad, M., Mustafa, A., Pietrzykowski, M., Frouz, J., 2023. Soil carbon storage in unreclaimed post mining sites estimated by a chronosequence approach and comparison with historical data. Catena 220A, 106664. https://doi.org/10.1016/j.catena.2022.106664

Zaiets, O., Poch, R.M., 2016. Micromorphology of organic matter and humus in Mediterranean mountain soils. Geoderma 272, 83–92. https://doi.org/10.1016/j.geoderma.2016.03.006

Zamanian, K., Pustovoytov, K., Kuzyakov, Y., 2016. Pedogenic carbonates: Forms and formation processes. Earth-Science Reviews 157, 1–17. https://doi.org/10.1016/j.earscirev.2016.03.003

Zanuzzi, A., Arocena, J.M., Van Mourik, J.M., Cano, A.F., 2009. Amendments with organic and industrial wastes stimulate soil formation in mine tailings as revealed by micromorphology. Geoderma 154, 69–75. https://doi.org/10.1016/j.geoderma.2009.09.014

Zasoński, S., Niemyska-Łukaszuk, J., 1977. Soil types of Mt. Zgorzelisko based on chemical and micromorphological properties, Roczniki Gleboznawcze – Soil Science Annual 28(1), 243–261.

Zikeli, S., Jahn, R., Kastler, M., 2002. Initial soil development in lignite ash landfills and settling ponds in Saxony-Anhalt, Germany. Journal of Plant Nutrition and Soil Science 165(4), 530–536. https://doi.org/10.1002/1522-2624(200208)165:4%3C530::AID-JPLN530%3E3.0.CO;2-J

Zwoliński, S., 1984. Wpływ hut zakopiańskich na lasy tatrzańskie. Parki Narodowe i Rezerwaty Przyrody 5(1), 43–50. (in Polish)

Mikromorfologiczne, submikromorfologiczne i chemiczne wskaźniki pedogenezy gleb technogenicznych w rejonach historycznego górnictwa i hutnictwa w Tatrach

Słowa kluczowe:

Gleby technogeniczne
Procesy glebotwórcze
Mikromorfologia gleb
Gleby górskie
Historyczne górnictwo
Historyczne hutnictwo

Streszczenie

Gleby technogeniczne (Technosols) powstałe z odpadów górniczych i hutniczych na obszarach historycznej działalności górniczej i hutniczej podlegają naturalnym procesom wietrzeniowym, glebotwórczym i biologicznym. W niniejszym artykule przedstawiono (1) wyniki badań mikromorfologicznych i submikromorfologicznych uzyskanych z użyciem mikroskopii optycznej i skaningowej mikroskopii elektronowej, a także (2) charakterystykę chemiczną opartą na wynikach selektywnych ekstrakcji pedogenicznych form Fe, Al, Mn i Si w glebach technogenicznych w Tatrach. Celem badań była identyfikacja procesów glebotwórczych zachodzących w tych glebach. Takie podejście pozwala na wgląd w złożoną pedogenezę gleb technogenicznych w środowisku alpejskim w obszarach, na które wpływ miała dawna działalność przemysłowa. Przeanalizowano trzynaście profili glebowych, podzielonych je na trzy grupy: (I) gleby technogeniczne utworzone z odpadów górniczych zawierających skały węglanowe (wapienie i dolomity) zawierające rudy żelaza i manganu, (II) gleby technogeniczne wytworzone z odpadów górniczych stanowiących skały magmowe i metamorficzne (granit, gnejs) z pozostałościami rud polimetalicznych, a także (III) gleby technogeniczne zawierające odpady z działalności hutniczej (np. żużle hutnicze). Analiza cienkich płytek (szlifów) z gleb ujawniła następujące mikroskopowe przejawy procesów glebotwórczych: (1) powstawanie pseudomorfoz tlenku żelaza w wyniku wietrzenia siarczkowego; (2) powstawanie pedogenicznej struktury; (3) tworzenie się pedogenicznych otoczek węglanowych w glebach utworzonych z odpadów górniczych zawierających skały węglanowe; (4) tworzenie się pedogenicznych otoczek zawierających tlenki żelaza i manganu w kwaśnych glebach utworzonych z odpadów górniczych składających się ze skał krystalicznych (granit, gnejs); (5) powstawanie pedogenicznych otoczek siarczanowych w glebach zawierających odpady metalurgiczne oraz (6) bioturbacje (np. kanały korzeniowe i kanały biogeniczne wypełnione materiałem przetworzonym przez faunę glebową). Obserwacje mikromorfologiczne wykazały również, że żużle metalurgiczne w glebach technogenicznych mogą stanowić siedlisko dla fauny glebowej (najprawdopodobniej nicieni lub wazonkowców). Selektywne ekstrakcje pedogenicznych form Fe, Al, Mn i Si wykazały (1) uwalnianie Mn ekstrahowanego szczawianem amonu w glebach wytworzonych z odpadów kopalnianych zawierających pozostałości rud Mn, (2) niewielką mobilizację Fe i Al ekstrahowanego szczawianem amonu w kwaśnych glebach technogenicznych wytworzonych z glinokrzemianowego materiału macierzystego oraz (3) uwalnianie Al i Si ekstrahowanych szczawianem amonu w glebach technogenicznych zawierających żużle hutnicze. Wyniki te wskazują, że technogeniczne materiały macierzyste podlegają procesom wietrzenia, które przekształcają skład mineralny badanych gleb technogenicznych. Niniejsza praca przyczynia się do poszerzenia wiedzy na temat gleb technogenicznych i ich potencjalnych funkcji ekologicznych w regionach górskich. Badania poszerzają również wiedzę na temat rozwoju gleb na obszarach historycznej działalności górniczej i hutniczej w środowisku alpejskim Tatr.